MEMBERSHIP OF THE ORION NEBULA POPULATION FROM THE *CHANDRA* ORION ULTRADEEP PROJECT

KONSTANTIN V. GETMAN,[1] ERIC D. FEIGELSON,[1] NICOLAS GROSSO,[2] MARK J. McCAUGHREAN,[3,4]
GIUSI MICELA,[5] PATRICK BROOS,[1] GORDON GARMIRE,[1] AND LEISA TOWNSLEY[1]

ABSTRACT

The *Chandra* Orion Ultradeep project (COUP) observation described in a companion paper by Getman et al. provides an exceptionally deep X-ray survey of the Orion Nebula Cluster and associated embedded young stellar objects. Membership of the region is important for studies of the stellar IMF, cluster dynamics, and star formation. The COUP study detected 1616 X-ray sources. In this study we confirm cloud membership for 1315 stars, identify 16 probable foreground field stars having optical counterparts with discrepant proper motions, and classify the remaining 285 X-ray sources, of which 51 are lightly and 234 heavily obscured. The 51 lightly obscured sources without known counterparts fall into three groups: (i) 16 are likely new members of the Orion Nebula Cluster; (ii) 2 with unusually soft and nonflaring X-ray emission appear to be associated with nebular shocks, and may be new examples of X-rays produced at the bow shocks of Herbig-Haro outflows; (iii) the remaining 33 are very weak uncertain sources, possibly spurious. Out of 234 heavily absorbed sources without optical or near-infrared counterparts 75 COUP sources are likely new embedded cloud members (with membership for 42 confirmed by powerful X-ray flares), and the remaining 159 are likely extragalactic active galactic nuclei seen through the molecular cloud, as argued by a careful simulation of the extragalactic background population. Finally, a few new binary companions to Orion stars may have been found, but most cases of proximate COUP sources can be attributed to chance superpositions in this crowded field.

Subject headings: binaries: general — open clusters and associations: individual (Orion Nebula Cluster) — stars: pre–main-sequence — X-rays: stars

On-line material: machine-readable tables

1. INTRODUCTION

The Orion Nebula Cluster (ONC), along with the Pleiades and Hyades, has served as the fundamental calibrator and prototype for young stellar clusters (O'Dell 2001). They are critical for understanding early stellar evolution, the stellar initial mass function, the dynamical history of clusters and multiple star systems, and the origins of planetary systems. The ONC has the best-characterized stellar population with age around 1 Myr (O'Dell 2001), and great efforts have been made to determine the cluster membership from its most massive member, the $\simeq 45\ M_\odot$ O7 star θ^1 Ori C, to substellar objects down to several Jupiter masses. Behind the ONC on the same line of sight lies the stellar population of the first Orion Molecular Core, OMC-1, which hosts the Orion hot molecular core and the nearest site of massive star formation (Kurtz et al. 2000). The stellar population of the ONC has been carefully identified by studies of proper motion (Jones & Walker 1988), optical spectra (Hillenbrand 1997), optical imaging (e.g., Prosser et al. 1994; Bally et al. 2000), infrared photometry (e.g., Hillenbrand & Carpenter 2000; Lada et al. 2004; M. J. McCaughrean et al. 2005, in preparation), infrared spectroscopy

(Slesnick et al. 2004), and radio continuum emission (Zapata et al. 2004). Over 2000 ONC members, and a score of embedded OMC-1 sources, are cataloged.

High-sensitivity and high-resolution X-ray surveys obtained with *Chandra* are also effective in detecting a large fraction of the Orion population, both in the lightly absorbed ONC and the heavily absorbed OMC-1 populations.[6] X-ray surveys are complementary to optical and infrared surveys because they trace magnetic activity (mainly plasma heated in violent magnetic reconnection flares) rather than photospheric or circumstellar disk blackbody emission. The survey methods thus have different sensitivities; for example, *Chandra* COUP sources can penetrate up to $A_V \simeq 500$ mag into the cloud, considerably deeper than existing near-infrared surveys in the *JHKL* bands. *Chandra* is also often effective in resolving multiple systems on arcsecond scales, as the mirror/detector system provide excellent dynamic range. Surveys in different bands are also subject to different types of contamination. Foreground and background Galactic stars confuse optical and near-infrared (ONIR) studies but have much less impact on X-ray studies, as magnetic activity in pre–main-sequence (PMS) stars is elevated 10^1–10^4 above main-sequence levels (Preibisch & Feigelson 2005). X-ray studies are thus particularly effective in uncovering heavily obscured low-mass cloud populations and in discriminating cloud pre–main-sequence populations from unrelated older stars. However, it is more difficult to remove extragalactic active galactic nuclei (AGNs) from high-sensitivity X-ray images—their X-ray properties can be similar

[1] Department of Astronomy and Astrophysics, 525 Davey Laboratory, Pennsylvania State University, University Park, PA 16802.

[2] Laboratoire d'Astrophysique de Grenoble, Université Joseph Fourier, BP 53, 38041 Grenoble Cedex 9, France.

[3] University of Exeter, School of Physics, Stocker Road, Exeter EX4 4QL, Devon, UK.

[4] Astrophysikalisches Institut Potsdam, An der Sternwarte 16, D-14482 Potsdam, Germany.

[5] INAF, Osservatorio Astronomico di Palermo G. S. Vaiana, Piazza del Parlamento 1, I-90134 Palermo, Italy.

[6] Other X-ray surveys are mentioned in the introduction to the first paper (Getman et al. 2005).

to those of absorbed PMS stars, and their number rapidly grows with increasing sensitivity of X-ray images. We carefully treat this problem here.

Two half-day exposures on the Orion Nebula obtained in 1999–2000 revealed 1075 X-ray sources; 974 were associated with known Orion stars, while 101 were unidentified X-ray sources, most of which were suspected new Orion members (Feigelson et al. 2002). A $\simeq 10$ day *Chandra* exposure of the Orion Nebula was obtained in 2003 January, providing the basis for the *Chandra* Orion Ultradeep Project (COUP).[7] The observations, data processing, source detection, photon extraction, and basic source properties are described by Getman et al. (2005). We discuss here the COUP findings with respect to the Orion stellar population.

One principal result is immediately evident: with $\simeq 10$ times the sensitivity of the earlier exposure, only 50% more sources are seen (1616 vs. 1075). We find few new lightly obscured members of the ONC, confirming the near completeness of earlier membership catalogs. COUP contributions to Orion population studies mainly involve heavily absorbed stars, which must be carefully discriminated from background AGNs based on their variability and spatial distributions (§ 2). A few sources may be nonstellar X-ray emission regions arising from shocks in Herbig-Haro outflows (§ 3). Double sources, a few of which may be physically related multiple star systems, are presented in § 4. Stellar contaminants unrelated to the Orion cloud are treated in § 5. A distance of 450 pc to the Orion Nebula is assumed throughout (O'Dell 2001).

2. DISCRIMINATING NEW CLOUD MEMBERS FROM EXTRAGALACTIC CONTAMINANTS

With the extremely deep net exposure of 838 ks, the COUP field undoubtedly suffers significant contamination by AGNs and other extragalactic sources. From megasecond exposures of the high Galactic latitude region (e.g., Brandt et al. 2001), we can estimate that $\simeq 500$–600 extragalactic sources would be detectable in the COUP field in the hard 2–8 keV band, which penetrates most cloud column densities. Thus, ideally without taking into consideration the molecular cloud distribution and even more importantly ignoring the effects of the complex elevated COUP instrumental background, about 30%–40% of the 1616 COUP sources are expected to be extragalactic contaminants. This is a much greater fraction than the $\leq 2\%$ contamination estimated for the shorter 1999–2000 *Chandra* exposures (Feigelson et al. 2002; Flaccomio et al. 2003) because the extragalactic source density climbs as $\log N \propto \log S^{-\alpha}$, where $1.0 < \alpha < 1.5$, while the ONC X-ray luminosity function is steeply declining below $\log L_t \sim 29$ ergs s^{-1} (Feigelson et al. 2002).

Here we apply a more sophisticated analysis of the extragalactic contamination than these rough estimates. First, the ONIR counterparts of Orion stars are nearly always brighter than the counterparts to extragalactic sources. Second, prior studies of the variability characteristics of AGNs and Orion population stars show that only the latter exhibit high-amplitude fast-rise flares. This criterion is more effective in the COUP study than in other *Chandra* observations of young stellar clusters because the long exposure improves the chances of capturing stellar flares. Third, we construct realistic Monte Carlo simulations of the extragalactic source surface density and flux distribution as a function of location in the COUP field, taking into account spectral properties of the AGNs, spatial variations in molecular cloud absorption and the variations in detector background peculiar to the

COUP field. The resulting predicted extragalactic populations are compared to COUP sources without ONIR counterparts.

2.1. *Candidate New Members*

Our consideration of extragalactic contaminants and new cloud members is restricted to the 285 COUP sources without known ONIR counterparts (see Tables 9 and 10 of Getman et al. 2005).[8] These 285 sources are listed in Tables 1 and 2, and their locations are plotted in Figure 1. The first nine columns of the tables give information extracted from the COUP source tables of Getman et al. (2005); see table notes for details. If the source lies in the Orion Nebula, a flux of $F_h = 1 \times 10^{-15}$ ergs s^{-1} cm^{-2} corresponds to a hard-band luminosity of $L_h = 2.3 \times 10^{28}$ ergs s^{-1}. Column (10) gives the column density through the molecular cloud derived from the velocity-integrated intensity of ^{13}CO from the single-dish map obtained by Bally et al. (1987). The ^{13}CO species is optically thin in most directions of the OMC (Bally et al. 1987), and therefore its brightness is a probe of the column density of molecular gas through the entire cloud. This map is shown in the background of Figure 1. The hydrogen column is estimated by the approximate correspondence of $A_V \sim 5$ mag to 5 K km s^{-1} and the conversion $\log N_H = 21.2 + \log A_V$ cm^{-2} (Vuong et al. 2003).[9]

Column (11) gives our proposed membership classification of these sources without ONIR counterparts as follows.

Orion Molecular Core (OMC).—These are 42 COUP sources without ONIR counterparts that exhibit one or more high-amplitude X-ray flares, a property characteristic of Orion cloud members but not extragalactic AGNs. These sources also exhibit two other properties not directly selected: they are all heavily absorbed ($\log N_H \geq 22.0$ cm^{-2}, and almost all are spatially associated with the dense OMC-1 cores, the dense molecular filament that extends northward from OMC-1 to OMC-2/3. We therefore classify these stars as members of the OMC and list them separately in Table 1.

Extragalactic (EG).—There are 192 heavily absorbed sources without ONIR counterparts that do not exhibit flares (Table 2). We establish in § 2.4 that most, but not all, of these are extragalactic sources. By comparing the observed and predicted local surface densities of these sources, in light of the requirement that extragalactic sources will be isotropically distributed, we provide in column (12) an estimated probability of membership. We label 33 of these sources "OMC or EG?" Most of these are probably new obscured Orion cloud members, leaving 159 probably extragalactic (EG) sources.

Orion Nebula Cluster (ONC).—There are 18 sources without ONIR counterparts that exhibit lower X-ray absorptions than expected if they lie in or beyond the molecular cloud. None of these exhibit X-ray flares. The nature of these sources is uncertain and is discussed in § 2.5. Two of them may be associated

---

[8] In Getman et al. (2005) the number of sources without known ONIR counterparts is actually 273, not 285. Five of the discrepant sources are explained here in § 4.2. For the remaining seven COUP sources (356, 577, 598, 635, 703, 704, and 748), their 2MASS registrations within the VLT field of view reported in Getman et al. (2005) were incorrect. As confirmed by VLT data, either 2MASS-*Chandra* separations are greater than 0″.8 and thus not considered to be true coincidences, or the 2MASS detection algorithm peaked on bright knots in the nebular emission rather than true stars.

[9] Vuong's relation, the latest published conversion between $\log N_H$ and A_V, is based primarily on data from ρ Oph cloud with only six data points from Orion, of which five have only moderate extinctions of $\log N_H < 21.8$ cm^{-2}. This relation has been extrapolated here to higher column densities. Examination of the $\log N_H - A_V$ relation up to $A_V \sim 200$ mag, the gas-to-dust ratio, and depletion effects is a future planned effort of the COUP project.

TABLE 1
FLARING COUP X-RAY SOURCES WITHOUT OPTICAL OR NEAR-INFRARED COUNTERPARTS

Source Number (1)	COUP J (2)	NetCts$_t$ (3)	NetCts$_h$ (4)	PSF (5)	MedE (keV) (6)	log N_H (cm^{-2}) (7)	kT (keV) (8)	F_h[a] (9)	log N_H OMC (cm^{-2}) (10)	Membership Class (11)
261....................	053506.1−052306	53.1	51.5	0.87	3.5	22.9	1.9	1.7	22.7	OMC
288....................	053507.4−052301	47.9	38.5	0.87	3.1	22.7	2.3	1.3	22.8	OMC
377....................	053510.4−052223	114.0	114.5	0.87	4.5	23.3	2.8	7.8	22.9	OMC
425....................	053511.5−052340	62.1	62.7	0.86	4.6	23.1	6.4	2.7	22.9	OMC
436....................	053511.6−052729	57.4	38.6	0.86	2.5	22.0	7.6	1.3	22.9	OMC
471....................	053512.2−052424	513.7	511.7	0.86	5.1	23.5	6.2	25.8	22.8	OMC
487....................	053512.6−052204	142.3	138.5	0.86	3.5	22.8	3.3	4.7	22.9	OMC
510....................	053512.9−052354	404.0	404.3	0.86	4.8	23.5	1.6	18.1	22.9	OMC
511....................	053512.9−052431	21.3	24.4	0.86	4.8	23.6	0.9	1.1	22.8	OMC
532....................	053513.2−052330	75.6	73.4	0.86	5.7	23.8	2.7	9.6	22.9	OMC
574....................	053513.7−052230	57.6	52.4	0.86	4.8	23.4	15.0	2.3	22.9	OMC
577....................	053513.8−052150	44.1	45.2	0.87	4.5	23.5	1.4	1.9	22.8	OMC
582....................	053513.8−052407	18.9	20.4	0.88	5.1	23.3	15.0	0.9	22.8	OMC
591....................	053513.9−052235	22.3	21.3	0.69	4.7	23.5	2.0	1.2	22.9	OMC
594....................	053513.9−052409	125.1	126.3	0.88	5.9	23.9	11.1	6.7	22.8	OMC
598....................	053514.0−052012	468.5	443.3	0.87	3.9	22.8	6.4	17.2	22.8	OMC
599....................	053514.0−052222	846.5	827.7	0.86	3.8	23.0	2.6	29.8	22.9	OMC
615....................	053514.2−052408	37.1	31.8	0.88	4.7	23.3	5.1	1.4	22.8	OMC
617....................	053514.2−052612	111.2	112.5	0.86	4.1	23.0	3.4	4.3	22.9	OMC
625....................	053514.3−052317	658.7	650.9	0.86	4.8	23.4	2.7	29.2	22.9	OMC
641....................	053514.5−052407	206.7	205.2	0.87	4.6	23.3	2.8	10.0	22.8	OMC
647....................	053514.6−052211	808.9	809.9	0.86	5.2	23.5	5.5	38.9	22.8	OMC
656....................	053514.7−052238	84.3	67.8	0.67	3.9	23.3	1.5	3.6	22.9	OMC
662....................	053514.8−052225	3270.8	3246.0	0.86	4.5	23.2	4.0	135.9	22.8	OMC
667....................	053514.8−052406	376.3	366.1	0.88	4.3	23.1	4.4	21.5	22.8	OMC
678....................	053515.0−052231	614.8	594.3	0.86	4.1	22.9	5.2	22.6	22.8	OMC
680....................	053515.1−052217	1384.3	1377.0	0.86	4.7	23.2	7.2	59.4	22.8	OMC
681....................	053515.1−052229	112.7	114.9	0.91	4.5	23.2	4.3	4.5	22.8	OMC
683....................	053515.1−052304	41.4	43.4	0.86	4.7	23.0	15.0	1.8	22.8	OMC
706....................	053515.4−052115	96.1	93.7	0.40	4.1	22.9	6.4	8.1	22.8	OMC
721....................	053515.6−051809	132.0	111.6	0.86	3.2	22.7	2.5	3.9	22.7	OMC
730....................	053515.7−051947	208.4	211.0	0.87	4.5	23.2	4.5	9.1	22.8	OMC
760....................	053516.0−051944	500.1	496.6	0.87	4.7	23.3	5.8	22.4	22.8	OMC
797....................	053516.3−052044	1716.0	1709.0	0.85	5.2	23.5	8.1	89.4	22.8	OMC
811....................	053516.5−052054	75.4	76.9	0.86	5.3	23.6	2.9	4.1	22.8	OMC
861....................	053517.1−052129	402.8	332.1	0.87	3.7	22.8	10.3	12.7	22.7	OMC
872....................	053517.3−052051	48.7	43.8	0.86	3.2	22.7	2.6	1.4	22.7	OMC
940....................	053518.0−052055	273.1	267.3	0.69	4.8	23.3	7.3	15.3	22.7	OMC
984....................	053518.6−051905	85.1	83.8	0.87	4.7	23.0	15.0	3.8	22.7	OMC
1051....................	053519.7−052110	170.9	166.3	0.86	4.2	22.8	15.0	6.7	22.6	OMC
1401....................	053527.9−051859	1565.5	1109.0	0.72	2.8	22.4	3.2	44.2	22.1	OMC
1465....................	053531.2−052215	56.3	54.1	0.87	3.8	23.0	2.4	2.1	22.4	OMC

NOTES.—Col. (1): COUP source number. Col. (2): IAU designation. Col. (3): Total band (0.5–8 keV) net counts in extracted area. Col. (4): Hard band (2–8 keV) net counts in extracted area. Col. (5): Fraction of the point spread function fraction in the extracted area. Col. (6): Median energy of extracted photons in the full band (corrected for background). Col. (7): Source hydrogen column density inferred from XSPEC spectral fit. Col. (8): Source plasma energy from the spectral fit. Col. (9): Observed hard band flux in units of 10^{-15} ergs cm^{-2} s^{-1}. Col. (10): Average hydrogen column density in OMC derived from the single-dish ^{13}CO map by Bally et al. (1987). Col. (11): Membership class derived here (§ 2.1). Table 1 is also available in machine-readable form in the electronic edition of the *Astrophysical Journal Supplement*.

[a] Units of 10^{-15} ergs s^{-1} cm^{-2} in the 2–8 keV band.

with Herbig-Haro outflows from Orion protostars, while the other 16 may be new very low-mass members of the ONC.

Herbig-Haro objects (HH).—COUP sees possible two cases in which the X-ray emission is unusually soft, constant, and faint and is associated with a nebular shock rather than a star. These are cases in which the bow shocks of high-velocity Herbig-Haro ejecta are sufficiently hot to produce soft X-rays.

Uncertain (Unc.).—There are 33 cases of lightly absorbed sources with ≲20 net counts. While the situation for these sources individually is uncertain, we suspect that, in most cases, the X-ray source detection is spurious and no source is actually present.

We now develop this classification in more detail.

2.2. K_s Band Magnitude Distributions

The star-galaxy discrimination benefits greatly by their disjoint distributions of ONIR magnitudes. This is best shown in the K_s band, where the VLT has covered the inner $7'.4 \times 7'.4$ of the Orion region to $K_s \simeq 20$ (M. J. McCaughrean et al. 2005, in preparation) and the 2MASS survey covers the outer region to $K_s \simeq 15$. In the ONC, the substellar limit occurs around $K_s \simeq 15$ (Muench et al. 2002) and only 14 COUP sources have counterparts with $16 < K_s < 20$ (Getman et al. 2005). In contrast,

TABLE 2

NONFLARING COUP X-RAY SOURCES WITHOUT OPTICAL OR NEAR-INFRARED COUNTERPARTS

Source Number (1)	COUP J (2)	NetCts$_t$ (3)	NetCts$_h$ (4)	PSF (5)	MedE (keV) (6)	log N_H (cm^{-2}) (7)	kT (keV) (8)	F_h[a] (9)	log N_H OMC (cm^{-2}) (10)	Membership Class (11)	P (12)
4......................................	053434.9−052507	16.5	57.8	0.89	5.0	23.4	1.4	2.9	22.3	EG	0.11
5......................................	053438.2−052338	68.6	60.0	0.69	4.7	23.5	9.5	3.9	22.1	EG	0.21
8......................................	053439.8−052456	1129.7	706.9	0.90	2.6	22.0	15.0	25.4	22.1	EG	0.06
18....................................	053443.4−052059	49.8	41.3	0.88	4.2	22.6	15.0	2.0	22.3	EG	0.56
19....................................	053443.9−052208	39.0	25.1	0.89	2.6	22.6	2.3	0.8	22.1	EG	0.51
22....................................	053444.5−052548	96.8	69.5	0.89	2.9	22.4	15.0	3.1	22.1	EG	0.31
24....................................	053445.3−052239	53.6	45.3	0.88	3.3	22.6	2.8	2.0	22.3	EG	0.50
25....................................	053445.4−052212	172.5	113.2	0.89	2.7	22.0	15.0	4.0	22.3	EG	0.59
31....................................	053446.7−052632	14.5	10.7	0.88	4.2	22.2	6.8	0.4	22.1	EG	0.03
32....................................	053446.8−052345	134.7	136.6	0.88	4.2	23.1	5.0	5.6	22.3	EG	0.22
34....................................	053447.2−052206	35.1	19.5	0.88	2.3	21.8	15.0	0.8	22.3	OMC or EG?	0.70
35....................................	053447.2−052307	199.2	141.5	0.87	2.8	22.3	6.8	5.3	22.3	EG	0.46
36....................................	053447.5−052128	152.2	121.8	0.89	3.3	22.5	3.7	5.1	22.4	OMC or EG?	0.66
38....................................	053448.0−052054	133.7	125.7	0.88	3.6	22.7	5.0	4.7	22.4	EG	0.38
39....................................	053448.1−052151	19.2	13.2	0.68	2.7	22.7	0.6	0.6	22.4	OMC or EG?	0.67
42....................................	053448.8−052118	42.1	40.9	0.88	4.0	23.4	1.4	1.6	22.4	EG	0.53
48....................................	053449.4−052359	69.1	56.9	0.88	4.0	23.5	1.1	2.6	22.4	EG	0.17
51....................................	053450.2−051854	120.9	94.0	0.78	3.3	22.3	15.0	4.0	22.4	EG	0.09
52....................................	053450.3−052323	231.2	178.4	0.89	3.3	22.3	15.0	7.4	22.4	EG	0.46
53....................................	053450.3−052631	13.5	4.9	0.48	1.4	20.0	10.8	0.4	22.3	ONC	...
56....................................	053450.7−052112	64.4	51.9	0.88	3.4	22.1	15.0	1.9	22.6	EG	0.28
61....................................	053451.4−052658	12.1	9.7	0.50	5.2	...	...	1.0	22.3	EG	0.00
63....................................	053451.5−052618	111.6	95.4	0.89	3.3	22.5	8.3	3.9	22.4	EG	0.02
70....................................	053452.4−051835	18.9	17.7	0.88	2.6	22.5	15.0	0.7	22.4	EG	0.00
76....................................	053452.9−052616	58.7	39.0	0.88	3.0	22.1	10.9	1.4	22.4	EG	0.06
81....................................	053453.3−052628	138.8	88.2	0.68	2.8	22.3	4.1	4.5	22.4	EG	0.00
82....................................	053453.4−052219	32.6	34.0	0.88	3.4	23.0	1.0	1.1	22.6	EG	0.45
83....................................	053453.5−052651	224.0	161.5	0.89	3.2	22.1	15.0	6.6	22.4	EG	0.00
84....................................	053453.8−052636	41.9	16.0	0.89	1.8	20.0	15.0	0.5	22.6	ONC	...
87....................................	053454.0−052501	41.7	26.1	0.88	3.2	22.0	15.0	1.1	22.6	EG	0.26
91....................................	053454.3−052207	79.1	69.1	0.88	4.1	23.0	15.0	3.0	22.6	EG	0.29
104..................................	053455.8−052338	201.2	186.9	0.87	3.8	22.7	8.6	7.3	22.6	EG	0.34
111..................................	053456.2−052229	999.2	849.2	0.87	3.5	22.5	10.4	32.5	22.6	EG	0.09
120..................................	053457.5−052346	63.5	47.2	0.88	4.1	23.0	15.0	2.0	22.6	EG	0.00
121..................................	053457.7−052223	285.2	261.3	0.88	3.8	22.6	15.0	10.2	22.6	EG	0.07
135..................................	053459.4−052251	14.6	2.2	0.88	1.1	20.0	1.6	0.1	22.6	ONC	...
136..................................	053459.4−052615	287.2	219.7	0.88	3.1	22.3	15.0	8.4	22.6	EG	0.20
138..................................	053459.6−052032	35.7	35.2	0.90	3.7	22.9	1.9	1.3	22.4	EG	0.00
145..................................	053500.2−052549	116.9	89.7	0.88	3.2	22.2	15.0	3.1	22.6	EG	0.08
146..................................	053500.4−051754	79.1	66.4	0.90	3.5	22.5	15.0	2.5	22.4	EG	0.00
151..................................	053501.1−052241	20.6	4.1	0.88	1.4	22.0	0.6	0.1	22.6	EG	0.30
156..................................	053501.2−052524	16.7	1.0	0.86	1.0	21.6	0.5	0.1	22.6	ONC	...
163..................................	053501.5−052158	98.9	87.3	0.86	4.0	22.8	4.3	3.4	22.6	EG	0.15
178..................................	053502.5−052601	20.9	18.5	0.88	3.7	22.4	15.0	0.7	22.6	EG	0.00
184..................................	053502.8−052628	23.0	17.5	0.90	3.5	21.9	15.0	0.6	22.6	Unc.	...
185..................................	053502.9−051551	339.8	118.4	0.87	1.6	21.8	1.3	8.8	22.6	ONC	...
186..................................	053502.9−053244	45.8	34.0	0.88	2.7	23.0	3.3	1.8	22.6	EG	0.00
191..................................	053503.2−053019	56.2	63.5	0.89	4.2	23.1	7.8	2.7	22.6	EG	0.00
196..................................	053503.5−052624	9.3	4.7	0.49	2.2	...	...	0.4	22.7	Unc.	...
198..................................	053503.6−052705	13.0	13.8	0.88	3.5	22.7	4.3	0.9	22.7	EG	0.00
203..................................	053503.9−052940	834.2	624.9	0.88	3.1	22.3	14.2	22.5	22.6	EG	0.00
204..................................	053504.0−052056	9.6	6.1	0.87	2.4	...	...	0.4	22.6	EG	0.00
225..................................	053504.7−052551	6.6	3.5	0.49	1.7	...	...	0.3	22.7	Unc.	...
229..................................	053504.8−052302	68.9	68.1	0.87	4.1	23.0	4.6	2.6	22.7	EG	0.02
257..................................	053505.8−053418	80.8	41.2	0.90	2.2	21.3	15.0	4.9	22.8	ONC	...
258..................................	053505.9−052550	16.0	12.1	0.90	3.3	22.5	2.6	0.4	22.7	EG	0.00
263..................................	053506.3−052336	197.7	184.9	0.87	4.0	22.7	15.0	7.1	22.7	EG	0.22
268..................................	053506.5−051624	70.0	55.4	0.88	2.9	22.1	15.0	2.2	22.6	EG	0.00
277..................................	053506.9−052244	15.6	16.3	0.87	3.5	22.8	1.4	0.6	22.7	EG	0.39
278..................................	053506.9−052421	7.4	2.1	0.50	1.9	...	...	0.1	22.8	Unc.	...
282..................................	053507.1−052650	28.7	25.8	0.87	3.2	22.3	15.0	0.9	22.8	EG	0.00
284..................................	053507.2−052253	111.0	114.4	0.86	4.9	23.4	9.6	5.6	22.7	EG	0.43
295..................................	053507.7−052626	13.0	8.9	0.86	2.3	20.0	15.0	0.2	22.8	Unc.	...
297..................................	053507.8−052029	86.2	82.6	0.87	4.1	22.8	15.0	3.3	22.6	EG	0.02

TABLE 2—*Continued*

Source Number (1)	COUP J (2)	NetCts$_t$ (3)	NetCts$_h$ (4)	PSF (5)	MedE (keV) (6)	log N_H (cm^{-2}) (7)	kT (keV) (8)	$F_h{}^a$ (9)	log N_H OMC (cm^{-2}) (10)	Membership Class (11)	P (12)
306	053508.3−051502	13.8	9.1	0.88	3.5	21.8	15.0	0.8	22.6	Unc.	. . .
317	053508.5−052501	18.4	18.9	0.86	5.0	23.5	10.5	0.8	22.8	EG	0.30
330	053509.2−051648	139.6	130.1	0.78	3.8	23.0	2.4	5.9	22.6	EG	0.00
354	053510.0−052004	95.0	91.0	0.87	3.8	22.8	4.3	3.3	22.6	EG	0.21
356	053510.0−052618	9.5	1.7	0.49	1.0	. . .	. . .	0.120	22.8	Unc.	. . .
360	053510.2−051719	53.3	49.1	0.88	5.1	23.6	3.6	2.5	22.6	EG	0.00
366	053510.2−052623	6.4	0.1	0.49	0.9	. . .	. . .	0.0	22.9	Unc.	. . .
381	053510.5−052003	68.9	63.5	0.87	3.7	22.6	15.0	2.5	22.6	EG	0.16
388	053510.5−053143	12.5	9.0	0.50	3.1	22.2	4.9	0.6	22.6	EG	0.00
400	053510.8−052804	39.9	6.5	0.38	1.2	21.5	1.1	0.5	22.8	ONC	. . .
402	053510.9−052227	80.6	74.4	0.87	4.1	22.8	8.9	4.0	22.9	OMC or EG?	0.81
406	053510.9−053006	26.3	24.9	0.68	3.7	22.8	2.8	1.2	22.7	EG	0.00
412	053511.1−052606	6.4	0.4	0.49	1.2	. . .	. . .	0.0	22.9	Unc.	. . .
451	053511.8−052403	4.5	2.5	0.50	2.2	. . .	. . .	0.2	22.9	Unc.	. . .
456	053511.9−052303	3.6	−0.8	0.86	1.0	. . .	. . .	. . .	22.9	Unc.	. . .
463	053512.1−052008	20.3	17.8	0.86	4.4	22.7	15.0	0.8	22.7	EG	0.32
473	053512.2−052600	6.9	2.8	0.60	1.7	. . .	. . .	0.1	22.9	Unc.	. . .
479	053512.4−052031	32.9	28.0	0.87	4.4	20.0	15.0	1.2	22.8	EG	0.54
495	053512.7−052254	16.0	4.3	0.86	1.4	20.0	15.0	0.1	22.9	ONC	. . .
496	053512.7−052410	11.5	13.0	0.86	5.2	23.3	15.0	0.7	22.9	OMC or EG?	0.71
505	053512.8−052247	12.7	7.8	0.86	3.8	20.0	15.0	0.4	22.9	OMC or EG?	0.84
506	053512.8−052342	8.8	7.0	0.60	4.8	. . .	. . .	0.6	22.9	OMC or EG?	0.83
508	053512.9−052254	5.8	6.0	0.50	4.3	. . .	. . .	0.4	22.9	OMC or EG?	0.89
509	053512.9−052330	40.7	39.3	0.86	5.1	23.4	15.0	3.6	22.9	OMC or EG?	0.89
521	053513.1−051809	16.3	1.2	0.87	1.2	21.6	0.8	0.1	22.7	Unc.	. . .
525	053513.1−052250	63.3	58.7	0.86	5.2	23.5	15.0	2.9	22.9	OMC or EG?	0.87
530	053513.2−052254	539.4	534.2	0.86	5.2	23.5	5.5	25.9	22.9	OMC or EG?	0.89
568	053513.6−053212	109.6	109.9	0.88	3.8	23.0	1.5	4.3	22.6	EG	0.00
571	053513.7−052147	37.2	39.0	0.87	4.6	23.2	15.0	1.6	22.8	OMC or EG?	0.73
575	053513.7−052438	12.4	11.2	0.86	4.1	. . .	. . .	0.9	22.8	OMC or EG?	0.73
581	053513.8−052246	14.1	8.9	0.68	2.5	22.5	1.1	0.3	22.9	OMC or EG?	0.88
589	053513.9−052229	60.0	57.6	0.68	3.7	23.3	1.3	2.6	22.9	OMC or EG?	0.91
601	053514.0−052313	9.0	4.4	0.47	2.3	. . .	. . .	0.3	22.9	Unc.	. . .
607	053514.1−052357	10.8	6.6	0.49	4.4	. . .	. . .	1.0	22.8	OMC or EG?	0.80
608	053514.1−052620	57.7	59.5	0.86	4.4	23.4	1.8	2.4	22.9	EG	0.00
611	053514.2−051804	64.0	64.9	0.87	3.9	23.0	1.4	2.5	22.7	EG	0.22
613	053514.2−052154	9.1	12.5	0.85	5.0	23.6	1.4	0.5	22.8	OMC or EG?	0.79
628	053514.4−052230	93.2	88.4	0.67	5.0	23.4	6.0	5.5	22.9	OMC or EG?	0.90
633	053514.4−052410	20.5	22.9	0.86	4.5	23.7	0.6	1.0	22.8	OMC or EG?	0.83
635	053514.4−052541	3.4	3.1	0.50	2.4	. . .	. . .	0.119	22.9	Unc.	. . .
637	053514.5−051956	20.1	6.5	0.89	1.7	21.5	5.6	0.2	22.8	Unc.	. . .
659	053514.7−052412	175.8	162.5	0.88	5.0	23.6	2.2	7.6	22.8	OMC or EG?	0.86
675	053514.9−052449	6.2	4.9	0.49	5.3	. . .	. . .	0.5	22.8	OMC or EG?	0.72
676	053514.9−052734	12.7	0.6	0.87	1.3	20.0	2.9	0.0	22.9	Unc.	. . .
692	053515.2−052509	6.9	4.1	0.49	2.1	. . .	. . .	0.3	22.8	Unc.	. . .
702	053515.4−051934	79.6	52.6	0.86	2.7	22.3	3.2	1.6	22.8	EG	0.54
703	053515.4−052040	32.0	4.6	0.87	0.9	21.9	0.1	0.101	22.8	HH	. . .
704	053515.4−052045	24.3	2.6	0.85	0.9	20.0	0.3	0.091	22.8	HH	. . .
709	053515.4−052507	69.1	65.7	0.86	4.8	23.2	15.0	3.0	22.8	OMC or EG?	0.70
723	053515.6−052126	585.1	580.0	0.87	4.8	23.2	15.0	25.7	22.8	OMC or EG?	0.64
748	053515.8−052417	8.7	4.3	0.87	2.3	. . .	. . .	1.690	22.8	Unc.	. . .
749	053515.8−052457	70.5	71.7	0.87	4.9	23.1	15.0	3.2	22.8	OMC or EG?	0.67
751	053515.8−053005	337.6	204.3	0.87	2.3	22.4	0.9	5.9	22.6	EG	0.00
755	053515.9−052200	319.2	322.4	0.87	4.7	23.3	3.3	14.0	22.8	OMC or EG?	0.71
767	053516.0−052334	35.2	7.9	0.49	1.2	20.0	2.0	0.4	22.8	Unc.	. . .
772	053516.0−052720	7.8	−1.2	0.86	1.2	. . .	. . .	. . .	22.8	Unc.	. . .
786	053516.2−052301	15.6	5.4	0.36	1.6	20.0	15.0	0.3	22.8	Unc.	. . .
793	053516.2−053332	107.3	98.5	0.74	3.7	22.8	4.7	4.9	22.6	EG	0.00
805	053516.4−051952	28.5	24.4	0.87	4.7	23.0	15.0	1.1	22.8	OMC or EG?	0.60
819	053516.6−052241	42.6	37.6	0.86	5.0	23.5	15.0	1.8	22.7	OMC or EG?	0.82
824	053516.7−052158	121.0	119.9	0.86	4.2	22.9	9.0	4.7	22.7	OMC or EG?	0.77
838	053516.9−051946	8.6	9.2	0.87	4.5	22.9	15.0	0.4	22.8	EG	0.58
846	053516.9−052302	14.2	1.4	0.36	1.2	21.1	1.2	0.2	22.7	Unc.	. . .
868	053517.2−052135	57.4	11.2	0.86	1.1	20.0	1.1	0.3	22.7	Unc.	. . .
877	053517.3−052240	17.2	12.3	0.90	2.1	. . .	. . .	0.2	22.7	Unc.	. . .

TABLE 2—*Continued*

Source Number (1)	COUP J (2)	NetCts$_t$ (3)	NetCts$_h$ (4)	PSF (5)	MedE (keV) (6)	log $N_{\rm H}$ (cm^{-2}) (7)	kT (keV) (8)	F_h[a] (9)	log $N_{\rm H}$ OMC (cm^{-2}) (10)	Membership Class (11)	P (12)
895............................	053517.5−052037	119.2	107.2	0.87	3.2	22.8	1.8	3.3	22.7	EG	0.53
905............................	053517.6−052233	8.7	0.1	0.41	1.3	...	...	0.0	22.7	Unc.	...
908............................	053517.7−051928	45.8	9.7	0.48	1.5	21.4	2.2	0.7	22.8	ONC	...
911............................	053517.7−052320	32.9	8.1	0.69	1.3	20.0	1.6	0.5	22.7	ONC	...
916............................	053517.8−051843	22.0	13.4	0.87	2.4	22.5	1.2	0.5	22.8	OMC or EG?	0.62
923............................	053517.8−052321	22.7	10.1	0.68	1.6	20.0	15.0	0.4	22.7	Unc.	...
933............................	053517.9−052326	18.1	4.2	0.68	1.2	21.7	0.6	0.2	22.7	Unc.	...
959............................	053518.2−052926	8.7	2.0	0.33	1.2	...	...	0.2	22.6	Unc.	...
961............................	053518.3−051501	119.8	77.4	0.87	2.6	22.1	15.0	3.4	22.6	EG	0.00
973............................	053518.5−051531	140.8	106.1	0.48	3.3	22.4	13.6	7.6	22.6	EG	0.00
975............................	053518.5−051929	14.8	11.4	0.87	4.2	22.1	15.0	0.5	22.7	OMC or EG?	0.75
1015..........................	053519.1−052112	143.1	131.3	0.87	3.6	22.8	2.3	4.5	22.6	EG	0.42
1016..........................	053519.1−052118	283.9	281.4	0.85	4.5	23.0	15.0	12.0	22.6	EG	0.45
1020..........................	053519.1−052528	3.1	1.9	0.47	2.3	...	...	0.1	22.8	Unc.	...
1031..........................	053519.3−053419	38.4	31.5	0.49	3.8	22.2	15.0	2.7	22.4	EG	0.00
1033..........................	053519.4−052716	14.2	8.2	0.87	2.6	21.3	15.0	0.3	22.7	ONC	...
1042..........................	053519.6−052057	45.3	31.7	0.87	2.6	21.9	15.0	0.9	22.6	ONC	...
1055..........................	053519.8−051841	27.3	20.2	0.88	3.1	...	...	0.7	22.7	EG	0.57
1057..........................	053519.8−052440	14.8	13.7	0.87	3.7	22.5	15.0	0.5	22.6	EG	0.52
1072..........................	053520.0−052223	8.0	5.6	0.49	2.1	...	...	0.3	22.6	EG	0.45
1078..........................	053520.0−052916	10.7	4.5	0.33	1.9	...	...	0.4	22.4	EG	0.00
1092..........................	053520.2−052706	13.8	4.2	0.87	1.3	20.0	1.9	0.1	22.7	ONC	...
1098..........................	053520.4−051932	195.8	186.4	0.86	3.7	22.8	5.3	7.0	22.6	OMC or EG?	0.72
1099..........................	053520.4−052019	14.3	10.3	0.88	3.5	23.4	0.6	0.4	22.6	OMC or EG?	0.65
1108..........................	053520.5−052425	26.2	21.8	0.87	4.1	22.5	15.0	0.9	22.6	EG	0.48
1109..........................	053520.5−052632	38.5	32.7	0.87	3.7	23.0	3.1	1.2	22.7	EG	0.22
1123..........................	053520.9−052234	312.4	291.0	0.86	4.1	22.7	15.0	11.5	22.4	EG	0.33
1133..........................	053521.0−052905	24.0	16.6	0.87	4.9	23.3	15.0	1.1	22.4	EG	0.00
1146..........................	053521.3−051902	39.5	36.3	0.87	3.5	22.6	3.8	1.5	22.6	OMC or EG?	0.60
1157..........................	053521.6−051754	33.4	23.3	0.88	3.2	20.0	15.0	0.8	22.6	EG	0.46
1176..........................	053521.8−052441	18.8	15.9	0.85	4.0	22.6	15.0	0.6	22.6	EG	0.30
1183..........................	053522.0−051933	33.5	37.8	0.86	4.2	23.0	4.7	1.6	22.6	EG	0.54
1189..........................	053522.1−052129	4.7	−2.4	0.87	1.1	...	...	...	22.4	Unc.	...
1192..........................	053522.1−052331	13.6	−0.9	0.87	0.9	21.1	0.3	...	22.4	ONC	...
1221..........................	053522.6−053338	76.7	75.3	0.59	3.7	22.7	4.5	4.6	22.1	EG	0.00
1228..........................	053522.7−052514	14.6	13.6	0.86	3.5	23.3	0.7	0.5	22.6	EG	0.23
1237..........................	053523.0−052459	799.9	56.0	0.86	1.0	20.0	0.6	1.7	22.6	ONC	...
1238..........................	053523.0−052836	26.7	−4.0	0.68	0.8	20.8	0.3	...	22.3	ONC	...
1254..........................	053523.5−051930	80.8	75.5	0.87	3.5	22.7	2.6	3.1	22.4	EG	0.57
1272..........................	053523.9−051913	6.2	4.3	0.48	3.2	...	...	0.311	22.4	EG	0.53
1283..........................	053524.3−052206	122.6	119.9	0.87	4.4	23.0	15.0	5.1	22.3	EG	0.23
1294..........................	053524.5−052526	6.4	2.0	0.47	1.3	...	...	0.102	22.6	Unc.	...
1304..........................	053524.7−052759	38400.3	27991.4	0.87	3.0	22.2	15.0	979.6	22.3	EG	0.22
1310..........................	053525.0−052326	262.5	214.9	0.87	3.4	22.4	15.0	8.2	22.4	EG	0.03
1315..........................	053525.1−052524	15.8	15.0	0.86	4.5	23.4	1.6	0.6	22.6	EG	0.29
1318..........................	053525.2−052823	8.4	6.3	0.47	2.3	...	...	0.3	22.3	EG	0.00
1325..........................	053525.4−052012	280.6	279.2	0.87	4.3	23.1	5.0	13.2	22.3	EG	0.33
1337..........................	053525.8−051809	7.3	3.6	0.33	2.3	...	...	0.4	22.3	EG	0.24
1339..........................	053525.9−053049	80.7	74.3	0.89	4.1	22.7	15.0	3.2	22.3	EG	0.21
1368..........................	053526.7−052013	84.6	80.3	0.87	3.8	23.0	2.8	3.2	22.3	EG	0.17
1375..........................	053527.0−052532	52.3	51.9	0.87	4.6	23.1	15.0	2.6	22.6	EG	0.01
1376..........................	053527.1−053002	55.2	43.7	0.88	3.3	22.4	15.0	1.7	22.3	EG	0.34
1377..........................	053527.2−052615	100.0	79.2	0.86	3.2	22.3	15.0	3.1	22.4	EG	0.12
1381..........................	053527.3−052928	16.9	6.0	0.77	1.7	22.5	0.5	0.2	22.3	EG	0.43
1383..........................	053527.4−051744	43.4	26.3	0.88	2.8	21.7	15.0	1.0	22.1	EG	0.06
1389..........................	053527.6−051816	42.6	42.2	0.88	3.6	22.8	2.9	1.5	22.1	EG	0.31
1395..........................	053527.7−052617	16.9	6.2	0.89	1.9	22.1	2.2	0.2	22.4	EG	0.21
1399..........................	053527.8−053109	370.4	232.5	0.87	2.5	22.2	6.2	8.5	22.1	EG	0.00
1420..........................	053529.0−052116	9.0	11.3	0.87	5.1	...	...	0.8	22.4	EG	0.05
1428..........................	053529.5−052311	24.3	20.7	0.87	3.4	22.4	15.0	0.8	22.3	EG	0.00
1437..........................	053529.9−052858	289.9	217.9	0.88	3.4	22.3	15.0	8.2	22.1	EG	0.32
1452..........................	053530.7−052535	5.1	3.6	0.48	2.4	...	...	0.2	22.4	EG	0.11
1453..........................	053530.7−052541	4.4	−0.4	0.50	1.4	...	...	...	22.4	Unc.	...
1460..........................	053531.0−052004	37.2	40.2	0.87	3.7	22.9	1.9	1.4	22.3	EG	0.12
1461..........................	053531.0−052428	8.6	4.8	0.50	2.8	...	...	0.4	22.4	EG	0.01

TABLE 2—*Continued*

Source Number (1)	COUP J (2)	NetCts$_t$ (3)	NetCts$_h$ (4)	PSF (5)	MedE (keV) (6)	log N_H (cm^{-2}) (7)	kT (keV) (8)	F_h[a] (9)	log N_H OMC (cm^{-2}) (10)	Membership Class (11)	P (12)
1467	053531.2−052725	66.0	47.0	0.87	2.9	22.5	2.9	1.5	22.1	EG	0.27
1471	053531.4−052136	375.2	222.1	0.87	2.3	22.2	2.6	8.2	22.4	EG	0.13
1476	053531.5−052245	21.7	24.1	0.87	5.0	23.6	1.5	1.2	22.3	EG	0.16
1482	053531.8−052230	27.8	22.7	0.87	3.0	22.9	1.2	0.7	22.3	EG	0.00
1486	053532.0−052945	149.4	110.4	0.88	2.8	22.2	5.6	3.6	22.1	EG	0.47
1491	053532.4−052822	223.1	150.4	0.88	2.8	22.0	15.0	6.1	22.1	EG	0.33
1493	053532.6−053047	17.0	13.3	0.88	4.0	...	...	0.7	22.1	EG	0.51
1494	053532.6−053125	19.8	14.9	0.20	3.4	22.3	15.0	2.7	21.6	EG	0.38
1498	053532.8−052222	21.1	21.2	0.87	3.8	23.3	0.7	0.8	22.4	EG	0.00
1502	053533.1−051846	37.9	17.9	0.87	2.0	21.9	1.5	0.9	22.1	EG	0.25
1504	053533.3−051651	194.8	165.0	0.88	3.7	22.4	15.0	6.6	21.6	EG	0.00
1505	053533.3−052720	54.3	26.7	0.88	2.0	21.4	15.0	1.2	22.1	EG	0.16
1506	053533.4−052702	293.9	200.9	0.87	2.7	22.3	3.8	6.8	22.1	EG	0.27
1509	053533.8−052244	7.4	4.7	0.68	2.5	...	...	0.2	22.4	EG	0.03
1510	053534.1−052541	14.4	16.9	0.88	3.9	23.2	1.5	0.6	22.3	EG	0.15
1515	053534.9−052836	62.5	42.6	0.88	2.8	21.9	15.0	1.5	22.1	EG	0.55
1518	053535.0−053035	182.7	163.5	0.89	3.2	22.4	5.6	5.7	22.1	EG	0.52
1527	053535.9−052531	42.1	35.8	0.87	3.5	22.5	15.0	1.4	22.3	EG	0.00
1528	053536.1−051913	36.9	28.0	0.87	2.6	22.6	1.1	0.8	22.3	EG	0.36
1530	053536.3−052427	7.6	6.2	0.49	4.9	...	...	0.6	22.3	EG	0.00
1536	053537.2−052004	22.9	19.9	0.88	2.7	23.1	0.6	0.6	22.4	EG	0.41
1538	053537.4−052324	20.8	15.6	0.89	2.9	22.2	5.1	0.7	22.4	EG	0.01
1541	053537.8−051826	120.4	103.0	0.88	3.6	22.9	3.5	4.0	22.1	EG	0.43
1545	053538.3−052540	21.2	18.9	0.88	3.4	22.6	2.7	0.7	22.3	EG	0.00
1548	053538.7−051858	9.9	16.0	0.88	4.2	...	...	0.5	22.3	EG	0.30
1551	053539.4−052854	154.3	97.6	0.88	2.6	22.2	5.8	4.5	22.1	EG	0.38
1552	053539.5−052842	14.5	7.1	0.49	1.8	21.7	4.0	0.5	22.1	EG	0.24
1554	053540.0−052016	221.7	225.5	0.87	4.2	22.9	15.0	9.7	22.4	EG	0.10
1555	053540.3−052840	56.6	46.8	0.88	3.5	22.4	15.0	1.7	22.1	EG	0.23
1556	053540.3−053013	120.8	88.2	0.87	2.9	22.5	2.8	6.3	22.1	EG	0.58
1559	053540.6−052807	127.3	101.3	0.88	3.3	22.4	15.0	4.1	22.1	EG	0.25
1565	053541.7−052015	385.3	300.5	0.88	2.9	22.5	2.5	10.0	22.4	EG	0.06
1575	053542.8−051930	42.7	37.5	0.88	3.7	22.4	15.0	1.6	22.3	EG	0.26
1578	053543.2−052759	154.2	104.4	0.87	2.6	22.2	4.3	3.6	22.1	EG	0.01
1580	053543.5−052119	67.6	68.8	0.88	4.2	22.5	15.0	2.9	22.3	EG	0.26
1581	053543.6−051928	63.3	49.2	0.89	3.8	22.6	15.0	2.6	22.3	EG	0.23
1582	053543.6−052400	91.2	82.4	0.87	3.8	22.7	7.3	3.4	22.3	EG	0.00
1583	053543.7−052637	12.5	10.2	0.49	4.0	...	...	1.0	22.3	EG	0.00
1586	053545.0−052233	23.5	20.1	0.89	3.4	22.6	3.2	0.7	22.4	EG	0.14
1589	053545.1−052255	31.3	34.0	0.89	4.5	...	...	1.5	22.4	EG	0.21
1597	053548.2−052357	14.1	15.5	0.88	3.6	23.4	0.5	0.6	22.3	EG	0.00
1598	053549.2−052417	115.3	114.6	0.88	4.0	23.0	2.4	4.8	22.3	EG	0.20
1600	053550.2−052139	43.9	54.9	0.88	4.7	22.9	15.0	2.5	22.4	EG	0.18
1601	053550.2−052211	19.3	13.7	0.68	2.9	22.0	15.0	0.8	22.4	EG	0.15
1605	053552.8−052713	96.0	82.2	0.88	3.2	22.2	15.0	3.1	22.3	EG	0.00
1606	053552.9−052305	50.4	38.4	0.89	3.7	22.8	4.6	1.8	22.3	EG	0.30
1607	053553.2−052603	698.8	554.5	0.89	3.0	22.4	5.6	22.7	22.1	EG	0.00
1609	053554.4−052436	346.0	258.1	0.89	3.1	22.2	15.0	10.3	22.1	EG	0.08
1615	053557.4−052415	151.6	122.0	0.89	3.2	22.6	4.0	5.2	22.3	EG	0.15

NOTES.—Col. (1): COUP source number. Col. (2): IAU designation. Col. (3): Total band (0.5–8 keV) net counts in extracted area. Col. (4): Hard band (2–8 keV) net counts in extracted area. Col. (5): Fraction of the point spread function extracted. Col. (6): Median energy of photons in the total band (corrected for background). Col. (7): Source hydrogen column density inferred from XSPEC spectral fit. Col. (8): Source plasma energy from spectral fit. Col. (9): Observed hard band flux in units of 10^{-15} ergs cm^{-2} s^{-1}. Col. (10): Average hydrogen column density in OMC from the ^{13}CO map by Bally et al. (1987). Col. (11): Membership class derived here (§ 2.1). Col. (12): Membership probability derived here (§ 2.4). Spectral results are unreliable for COUP 84, 257, 495, and 1033 because the fitting procedure failed due to substantial hard-band contamination. Spectral results are unreliable for COUP 479, 505, and 1157 because the fitting procedure failed due to substantial soft-band contamination. Table 2 is also available in machine-readable form in the electronic edition of the *Astrophysical Journal Supplement*.

[a] Units of 10^{-15} ergs s^{-1} cm^{-2} in the 2–8 keV band.

for extragalactic X-ray populations only ∼1% have counterparts with $K_s < 18$ (Barger et al. 2002), and most of these are resolved galaxies.

We are therefore confident that very few (<10 and possibly zero) of the COUP sources with ONIR counterparts listed by

Getman et al. (2005) are extragalactic. Nearly every COUP source with an optical or NIR counterpart will be a true member of the ONC, an obscured member of the background molecular cloud, or possibly a foreground or background interloper from the Galactic field star population.
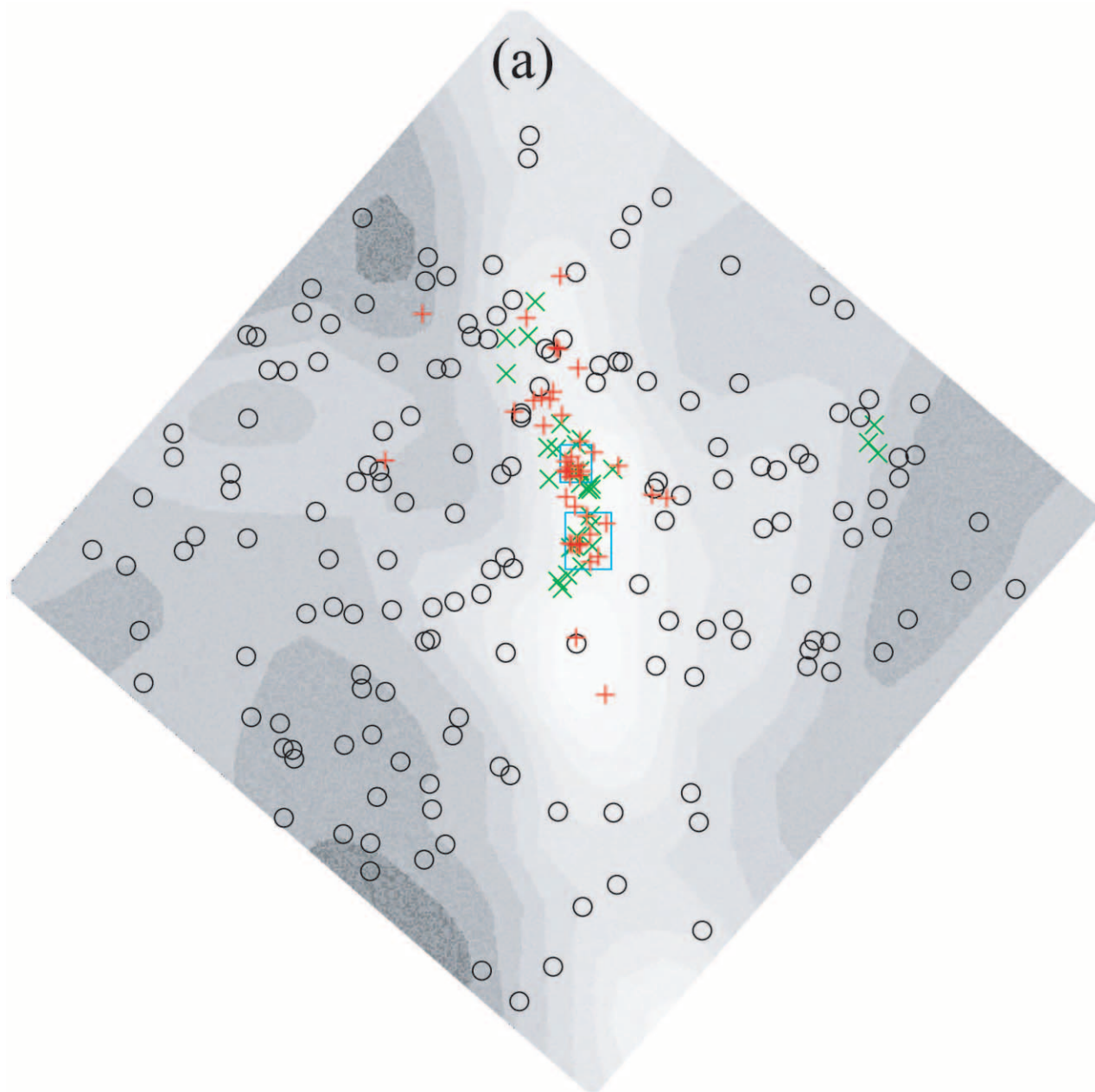
Fig. 1.—Locations of hard (=absorbed) COUP sources without optical or near-infrared counterparts are plotted on a map of molecular line emission in the Orion Nebula region: (a) the full $17' \times 17'$ COUP field centered at $(\alpha, \delta) = (83.82101, -5.39440)$; and (b) a close-up of the $5' \times 10'$ OMC-1 cores region. Two small cyan boxes indicate BN/KL and OMC1-S regions discussed in detail by Grosso et al. (2005). Forty-two flaring unidentified X-ray sources are marked by red pluses. From 192 hard unidentified nonflaring COUP sources, 159 classified as extragalactic are marked by black circles, and 33 likely additional cloud members are marked by green crosses. Both the 42 flaring and 33 nonflaring sources cluster around the OMC cores.

2.3. Flaring Members

Perhaps the most definitive criterion for distinguishing young Orion stars from background objects is the presence of strong X-ray flares. These typically have rise times ≤ 1 hr and decay times of 10–100 hr, though a wide diversity of flare morphologies is seen (Wolk et al. 2005). This flare emission is attributed to plasma trapped in closed magnetic structures and violently heated by magnetic reconnection events (Favata et al. 2005). Such X-ray flares are not expected to be seen either from older background main-sequence stars that are 10^1–10^4 times less powerful than Orion stars or from extragalactic AGNs, which typically exhibit slow and mild variability over the $\simeq 2$ week COUP exposure time (Bauer et al. 2003; Paolillo et al. 2004).

Based on results of the Kolmogorov-Smirnov and Bayesian Blocks analysis described by Getman et al. (2005), and visual inspection of source light curves and photon arrival diagrams, we find that 42 of 285 unidentified sources have strong flares characteristic of Orion stars. To quantify their variability, all 42 have $\log P_{KS} < 2$ or BBNum ≥ 2, and all except three (COUP 582, 656, 678) have BBmax/BBmin > 4 (Getman et al. 2005, § 8). These 42 sources are classified as OMC (i.e., Orion Molecular Cloud members) in Table 2, and their light curves are shown in Figure 2.[10]

[10] In addition, OMC membership for COUP 678 and 681 is confirmed by Grosso et al. (2005), who report that they are associated with anonymous NICMOS sources in the image of Stolovy et al. (1998).
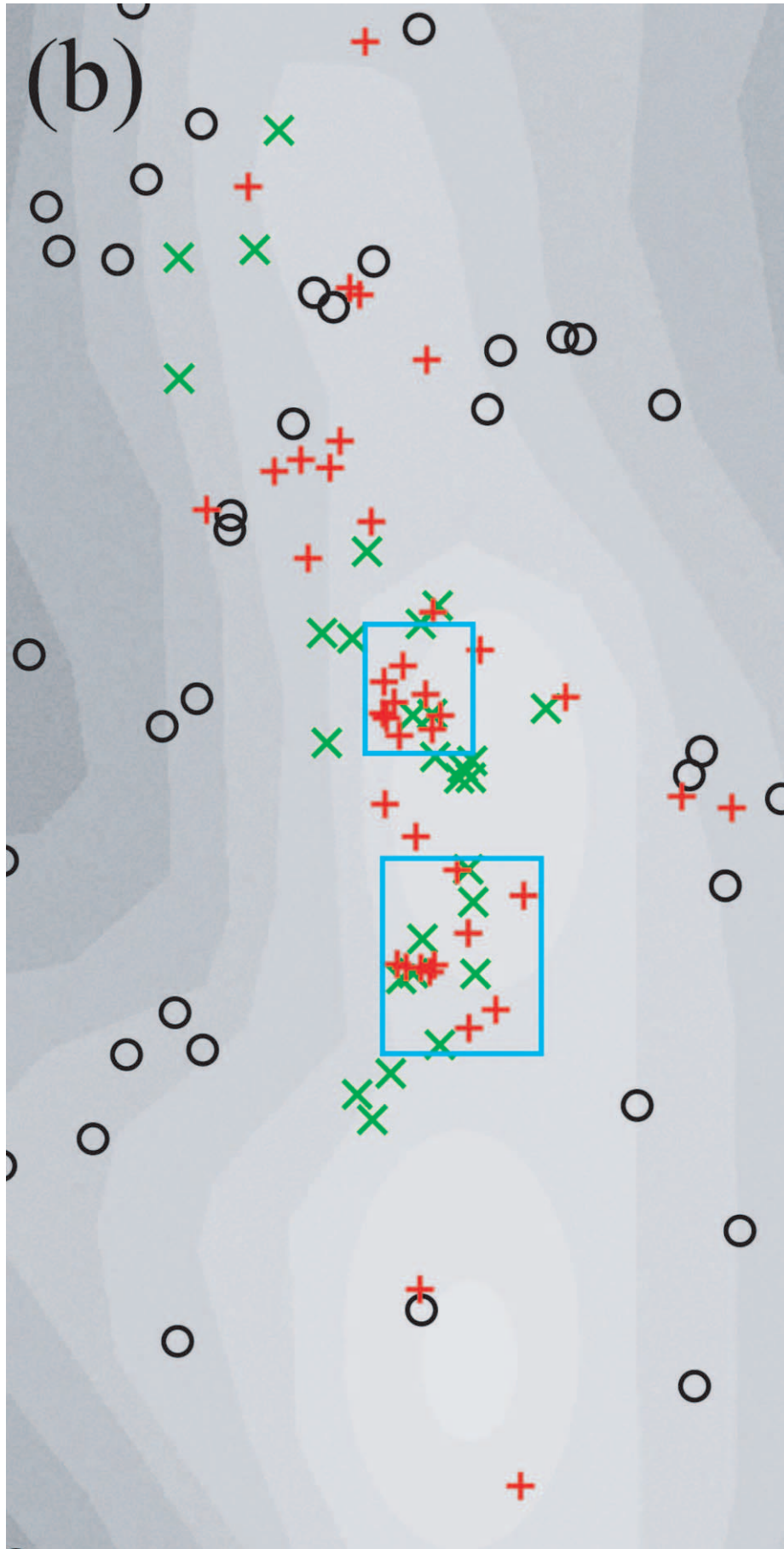
Fig. 1.—*Continued*
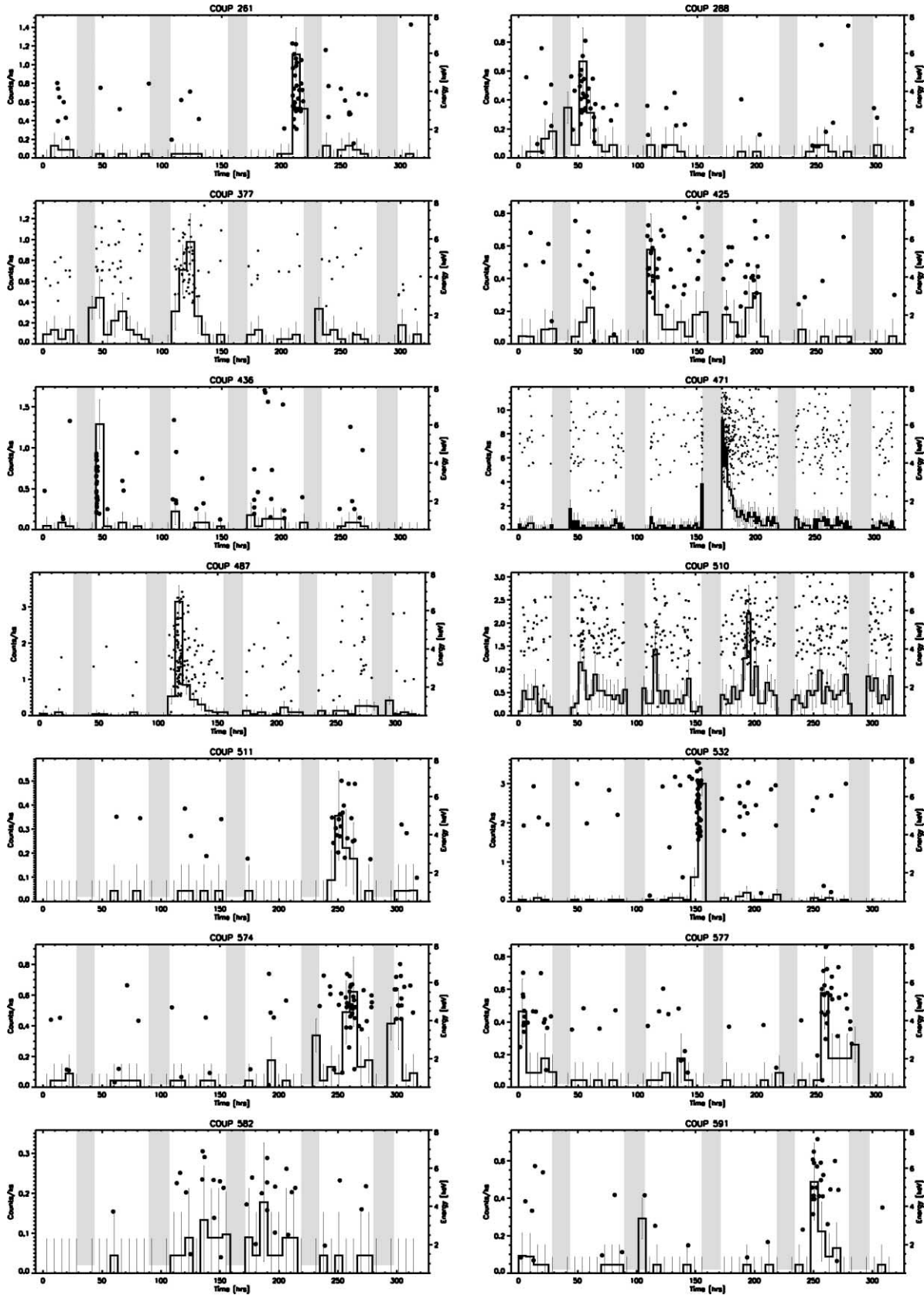
FIG. 2.—Light curves (*line*) and photon arrival diagrams (*dots*) for 42 X-ray flaring newly discovered members of the Orion Nebula region. The histograms show binned count rates (*left ordinate*) in the total (0.5–8.0) keV energy band. Dots show individual photon arrival times with vertical position indicating their photon energies (*right ordinate*). Abscissae show the time after the beginning of the COUP observation in hours. Gray bars indicate the time gaps in the COUP exposure due to perigees of the *Chandra* satellite orbit.

COUP 594 · COUP 598 · COUP 599 · COUP 615 · COUP 617 · COUP 625 · COUP 641 · COUP 647 · COUP 656 · COUP 662 · COUP 667 · COUP 678 · COUP 680 · COUP 681
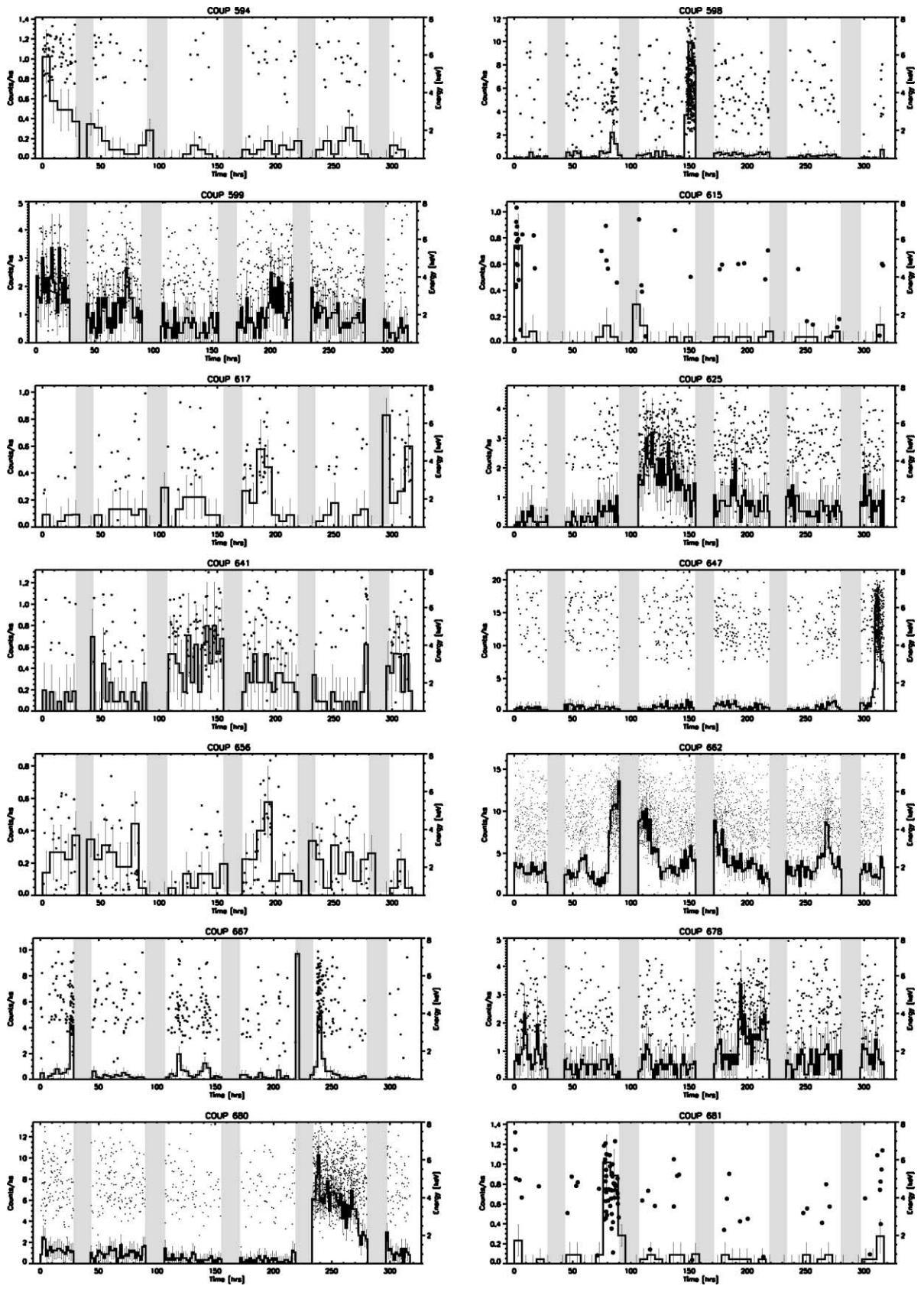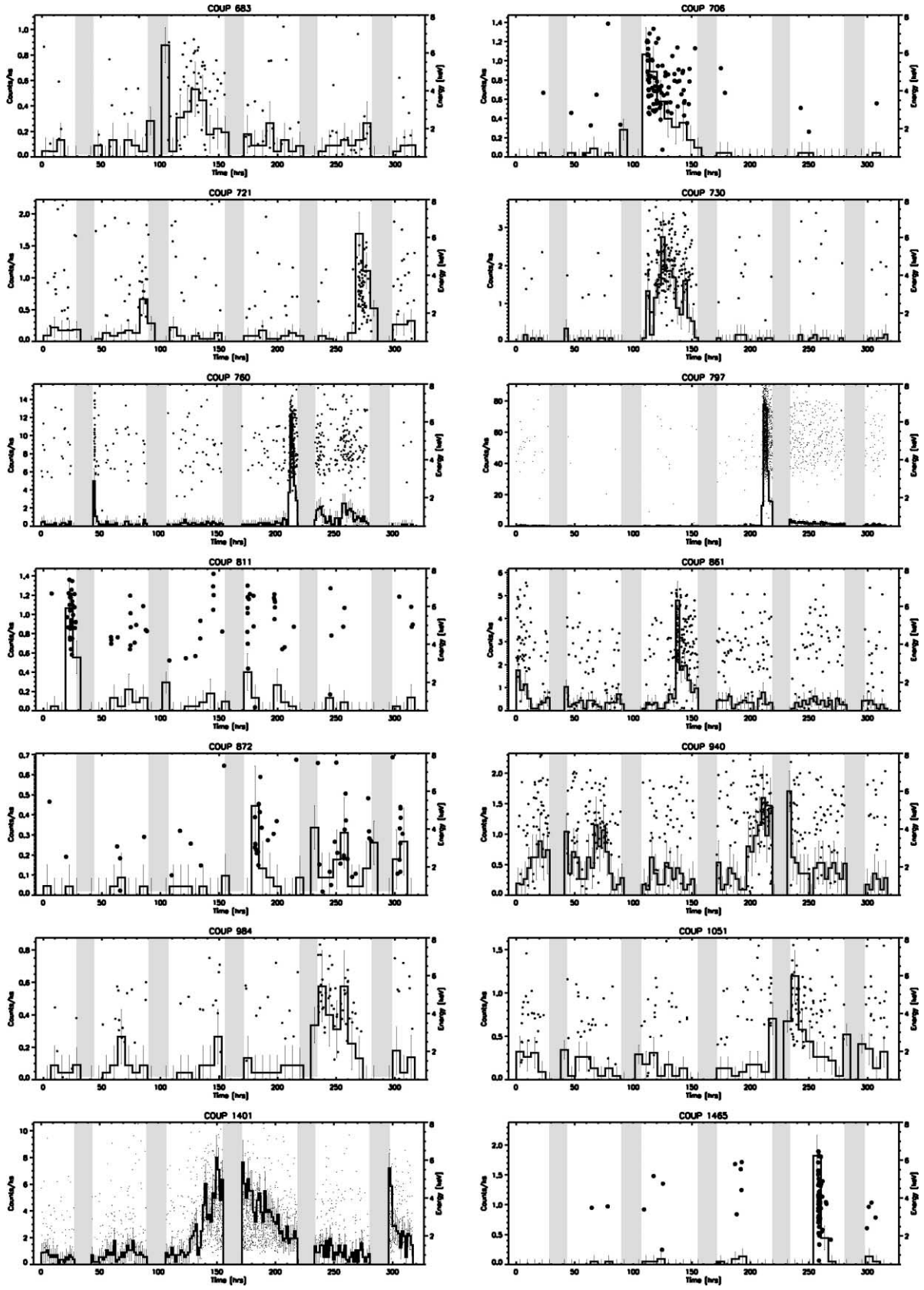
FIG. 2.—*Continued*

FIG. 2.—*Continued*

Although these sources were selected only on the basis of flaring light curves, they exhibit two additional indicators of cloud membership. First, their spatial distribution is strongly clustered around the dense OMC-1 cores (Fig. 1), inconsistent with the expected distributions of unrelated stellar or extragalactic populations. Second, the absorbing column densities derived from XSPEC spectral fits for the 42 flaring sources (median $\log N_H \sim 23.2$ cm^{-2}) are very high, excluding the possibility that they lie in front of the cloud cores. Indeed, their X-ray absorptions appear systematically higher than the average depth in OMC cores [median $\log N_H(^{13}CO) \sim 22.8$ cm^{-2}]. This may be explained by poor resolution of ^{13}CO maps or inaccurate conversion between ^{13}CO and total hydrogen columns but, if real, may indicate that these sources are very young with the local absorption in an envelope or disk.

2.4. *Extragalactic Population Simulations*

To evaluate the expected contamination of extragalactic X-ray sources in the COUP ACIS-I field, we constructed Monte Carlo simulations of the extragalactic population by placing artificial sources randomly across the field. The entire analysis of this subsection is confined to the COUP hard band (2–8 keV). The incident fluxes of individual simulated sources were drawn from the observed X-ray background $\log N - \log S$ distribution described by Moretti et al. (2003), assuming a power-law photon index distribution consistent with flux-dependencies described in Table 3 of Brandt et al. (2001). The spectrum of each individual simulated source was convolved with absorption obtained from the ^{13}CO column map shown in Figure 1 at the source position. To account for the observed COUP background for each simulated source, which is nonuniform due to the readout trails and highly populated wings of bright ONC X-ray sources, we applied the background noise from the location of the nearest COUP source (reported in Table 4 of Getman et al. 2005) and removed very weak extragalactic sources when they would not have been detected above the local background level. The resulting detection threshold ranged from 3.3 to 5.0 times the root mean square local noise level, representing the signal-to-noise range of the faintest COUP sources.

The results of a number of such simulations in the form of a $\log N - \log S$ X-ray source surface density plot are shown as a gray band in Figure 3. A range of 140–240 extragalactic sources are predicted to have been detected by the COUP processing, which agrees well with the observed sample of 192 hard-band COUP sources without ONIR counterparts (in Table 2; Fig. 3, *upper solid line*). Considering only the total population, these results are consistent with no new Orion cloud members among the 192 sources.

However, we also know the spatial distribution of both the observed unidentified COUP sources and the predicted extragalactic population in each simulation. About 15% of the 192 sources are clustered in the immediate vicinity of the dense OMC-1 cores, where most of the new 42 X-ray flaring members are found (Table 1). This region has a $\simeq$4-fold higher concentration of unidentified sources than the rest of the COUP field ($\sim$2–3 vs. 0.5–0.8 sources arcmin^{-2}). This is precisely the region in which the simulated extragalactic populations have a deficit of sources due to heavy absorption by the molecular cloud cores.

To identify these clustered sources in an objective fashion, we applied an adaptive kernel smoothing algorithm to both the simulated extragalactic population and the 192 unidentified hard COUP sources. The kernel width was chosen to accumulate at least 10 COUP sources around each source, resulting in kernel areas $\sim$2 arcmin^2 in the center of the field and larger toward the edges. We define an approximate membership probability for
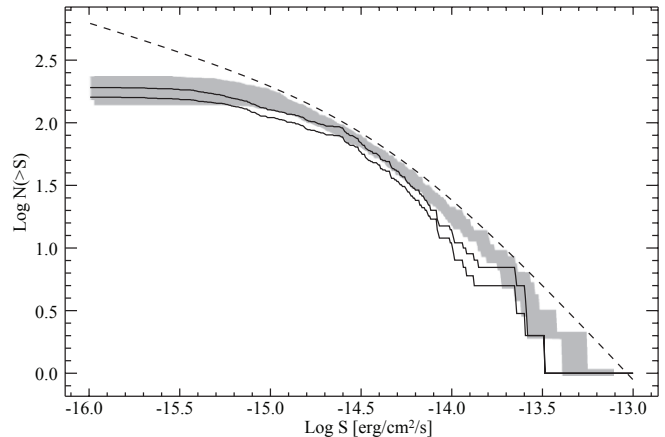
FIG. 3.—Evaluation of extragalactic source contamination using the X-ray source $\log N - \log S$ diagram. N gives the number of sources seen or calculated in the COUP field of view as a function of source flux in the hard 2–8 keV band. *Upper solid line*: Observed flux distributions of the 192 heavily absorbed nonflaring COUP sources without ONIR counterparts (EG and "OMC or EG?" sources in Table 2). *Lower solid line*: Same for the 159 sources with low probability of cloud membership (EG sources only). *Dashed line*: Expected unobscured extragalactic $\log N - \log S$ distribution (Moretti et al. 2003). *Gray band*: Range of simulated distributions of this extragalactic population for the COUP field corrected for source spectral variations, spatially variable absorption by the Orion Molecular Cloud, and variations in the COUP background.

each observed source $P = (N_{COUP} - N_{AGN})/N_{COUP}$, where N_{COUP} is the number of hard unidentified COUP sources around the current COUP source within the kernel area and N_{AGN} is the number of expected simulated AGNs within the same kernel area averaged over the simulations and assuming a 4.4 σ detection threshold. These membership probabilities are listed in column (12) in Table 2. The concentration around the OMC-1 cores corresponds roughly to $P \geq 0.60$, and we use this criterion to define the "OMC or EG?" classification in the table and Figure 1.

The $P = 0.60$ threshold is clearly ad hoc and is unlikely to provide a clean discrimination between cloud members and extragalactic AGNs. Nonetheless, we suspect that most of the 33 "OMC or EG?" sources are in fact new obscured Orion cloud members similar to the OMC flaring sources in Table 1. The "OMC or EG?" sources (Fig. 1, *green crosses*) are also spatially clustered around the OMC-1 cores similar to the 42 new flaring sources (*red plus signs*). The median column density of the 33 sources is $\log N_H \sim 23.3$ cm^{-2}, nearly identical to that of flaring sources, but with fewer counts (median of 43 counts vs. 114 for the flaring sources). The "OMC or EG?" sources are either too weak to show flares, or happened not to exhibit a powerful flare during the COUP observation.

In this case, the contaminating extragalactic AGN population is restricted to be no more than 159 sources (192 minus 33 probably OMC members) in Table 2. These sources are distributed across the field in a roughly random fashion except for the expected avoidance of the absorbing cloud cores (Fig. 1). Their $\log N - \log S$ distribution is reasonably consistent with the extragalactic population simulations (Fig. 3).

2.5. *Lightly Absorbed COUP Sources without ONIR Counterparts*

About one-fifth of the sources in Table 2 have X-ray absorptions that appear to be significantly below values expected if they lie deeply embedded in or behind the Orion molecular cloud. A rough criterion for this would be $\log N_H < \log N_H(^{13}CO) - 0.6$ cm^{-2}, where 0.6 is the typical uncertainty on logarithm N_H seen in Table 6 of Getman et al. (2005). We consider the 18 of

these sources with $\log N_H < 22.0 \text{ cm}^{-2}$ to be "lightly absorbed"; 8 of these have $\log N_H \leq 20.0 \text{ cm}^{-2}$, which is the lower limit of absorption detectable with the *Chandra* instrument. We thus consider these 18 sources to lie in front of (or only slightly embedded in) the molecular cloud. Since most of the ONC similarly lies in front of the cloud with only light absorption (O'Dell 2001), we tentatively classify 16 of these sources as ONC members and 2 as possible HH objects (see § 3) in Table 2.

However, the ONC class is probably not homogeneous, and we consider several separate subclasses.

1. Five of the sources (COUP 53, 135, 156, 1033, and 1092) are weak X-ray sources with <20 net counts located out of the VLT field of view. From the $L_t - L_{bol}$ relationship (Preibisch et al. 2005), their photospheric brightness can easily be below the $K_s \simeq 15$ 2MASS completeness limit. These are likely new low-mass members on the outskirts of the ONC.

2. Two cases may represent associations between the X-ray position and known ONIR cluster members that were missed by the automated source identification procedures of Getman et al. (2005). COUP 185 and 257 are located at edges of the COUP field so the centroid of these point spread functions cannot be accurately found. They are probably associated with V403 Ori (13″ to the northwest) and V387 Ori (14″ to the southwest), respectively.

3. Five cases (COUP 84, 400, 908, 1237, and 1238) lie very close to known ONC members and may be new binary companions. See § 4 for details.

4. Four cases (COUP 495, 911, 1042, and 1192) are located within the VLT field of view. COUP 911 is a very faint X-ray source lying 23″ east-northeast of θ^1 Ori C; it may be a new very low-mass ONC member. COUP 1042 is a very faint X-ray source lying 10″ west of the $V \simeq 12$ classical T Tauri G star TU Ori, which is already known to have a flare star companion (Hambarian 1988). The nebular emission is bright in these regions, perhaps inhibiting VLT detection of an X-ray–emitting low-mass ONC member.

Finally, we find that the remaining 33 of 51 unidentified unabsorbed sources are very weak ($\lesssim 20$ net counts in all cases and <10 net counts in most cases), have low source significance, are undetected with the PWDetect source detection algorithm and (for 27 of the 33) flagged as "uncertain" source existence in Table 2 of Getman et al. (2005). We indicate their class as "Unc." here in Table 2. We suspect that their identification as X-ray sources by the procedures described in Getman et al. was mistaken and that most of these are not real X-ray sources.

3. X-RAY SOURCES ASSOCIATED WITH NEBULAR SHOCKS

Two sources, COUP 703 and 704, are very faint, show constant X-ray light curves without flares, have unusually soft ACIS spectra, and have no ONIR stellar counterpart. They coincide with HH 210, which is one of the fingers of the molecular flows emerging from the massive star(s) in the Orion hot molecular core. These are likely new discoveries of X-ray emission from Herbig-Haro outflow bow shocks, similar to those seen in the HH 1/2 and HH 80/81 outflows (Pravdo et al. 2001, 2004). We designate these sources as HH in Table 2. The difference between $\log N_H \sim 21.9 \pm 0.2 \text{ cm}^{-2}$ of COUP 703 and $\log N_H \sim 20.0 \pm 2.5 \text{ cm}^{-2}$ of COUP 704 can be explained by the high uncertainty of the column density for COUP 704 (see Table 6 of Getman et al. 2005). Accurate astrometry study and details regarding X-ray emission from HH 210 will be presented in N. Grosso et al. (2005, in preparation).

4. DOUBLE SOURCES

4.1. *Double X-Ray Sources with Separations* <3″

The ONC is an important laboratory for investigating the origin and evolution of binary star systems. For binaries with separations $\simeq 25$–500 AU ($\simeq 0\farcs 06$–1$\farcs$1), the ONC has been shown to be strongly deficient in binaries compared to low-density star formation regions such as the Taurus-Auriga clouds with a binarity fraction similar to that seen in main-sequence field stars (see Prosser et al. 1994, Padgett et al. 1997, Petr et al. 1998, and the review by McCaughrean 2001).

Searches for wide binaries are dominated by chance superpositions of stars in the crowded cluster core. No wide binaries with 1000–5000 AU (2$\farcs$3–11″) separations are found among $M \geq 0.2 \, M_\odot$ cluster members when random coincidences and proper motions are taken into account (Scally et al. 1999). In contrast, 15% of field stars are binaries in this range (Duquennoy & Mayor 1991). Wide binaries are dynamically fragile and may be disrupted by gravitational encounters with nearby stars. *N*-body simulations of the ONC indicate that most wide binaries will be quickly ($t < 0.4$ Myr) disrupted if the cluster is in virial equilibrium, but many should have survived if the cluster is expanding due to ejection of natal molecular gas (Kroupa et al. 1999). The census of wide binaries in the ONC thus gives valuable information regarding the dynamical history of the cluster.

The COUP sample of X-ray–emitting stars in the ONC provides a new capability for measuring ONC wide binaries for three reasons. First, the sample has different selection effects than traditional optical samples: COUP measures magnetic activity rather than bolometric luminosity diminished by obscuration. This results in several dozen new pre–main-sequence members, though most of these are heavily obscured in the cloud behind the cluster core (§ 2.3). Second, it is sometimes easier to detect a lower mass companion to a higher mass primary in X-rays because the contrast in X-ray luminosities is smaller than in bolometric luminosities. This is particularly true for intermediate-mass ($1.5 \, M_\odot < M < 10 \, M_\odot$) primaries. Finally, a statistical link between binarity and X-ray emission has been reported in main-sequence field stars (Makarov 2002), which would assist in the detection of new companions, though no such effect has been found in the Taurus-Auriga pre–main-sequence population (König et al. 2001).

Table 3 lists the 61 pairs of COUP sources lying within 3″ of each other. The closest pair has separation 0$\farcs$7, but the minimum detectable separation is a function of off-axis location in the *Chandra* field. The first six columns of the table give X-ray information from Getman et al. (2005), the next four columns give JHK_s and optical-band counterparts from Getman et al., and the last two columns give membership classification based on results obtained in this study. The lower COUP sequence number always refers to the western (W) component of the double.

Small "postage-stamp" images of these 61 doubles are shown in Figure 4. For each pair we give the original COUP data (*top panel*), a maximum-likelihood reconstruction of the region (*middle panel*), and a reproduction of the best available K_s-band image (*bottom panel*). The reconstruction was performed using the Lucy-Richardson algorithm (Lucy 1974) with 100–200 iterations based on the local *Chandra* point spread function generated by the CIAO program `mkpsf`. The procedure is run within the `acis_extract` data reduction environment[11] (Getman et al.

---

[11] Descriptions and codes for `acis_extract` can be found at http://www .astro.psu.edu/xray/docs/TARA/ae_users_guide.html.

TABLE 3
COUP DOUBLE SOURCES WITH <3″ SEPARATIONS

		X-RAY SOURCES				OPTICAL/NEAR-INFRARED SOURCES					
COUP (W) Number (1)	COUP (E) Number (2)	Separation (arcsec) (3)	Off-Axis (arcmin) (4)	MedE (W-E) (keV) (5)	$\log N_{\rm H}$ (W-E) $({\rm cm}^{-2})$ (6)	IR (W) (7)	Opt. (W) (8)	IR (E) (9)	Opt. (E) (10)	Class (W) (11)	Class (E) (12)
57..................	59	2.1	6.6	1.1–1.1	20.7–20.8	2MASS	116	. . .	10281	M	M
74..................	75	2.2	7.4	1.3–1.4	21.4–21.8	2MASS	137	2MASS	136	M	M
123................	124	1.4	4.8	1.5–1.4	21.2–21.1	2MASS	176	2MASS	176	M	M
213................	214	0.9	3.2	1.1–1.5	20.9–20.6	51	. . .	53	248	M	M
251................	252	2.3	3.1	1.0–1.3	20.0–20.9	103	275b	102	275a	M	M
283................	286	3.0	2.7	1.3–1.0	21.1–20.0	141	300	143	302	M	M
315................	316	1.7	2.3	2.7–1.1	22.5–21.3	174	. . .	172	322	M	M
374................	375	2.1	2.7	1.8–2.0	21.6–22.3	235	. . .	231	. . .	M	M
378................	384	1.8	1.9	1.2–1.4	21.1–21.2	238	345	244	350	M	M
403................	408	2.1	1.8	3.2–2.7	22.5–22.4	261	355	266	10415	M	M
425................	442	2.8	1.4	4.6–1.1	23.1–20.0	. . .	. . .	296	9008	NM	M
440................	441	3.0	1.3	4.8–3.9	23.2–23.0	297	. . .	299	. . .	M	M
495................	508	2.7	1.3	1.4–4.3	20.0–. . .	. . .	. . .	. . .	. . .	NM?	NM?
503................	504	0.7	2.3	3.4–3.2	22.7–22.6	346	. . .	344	. . .	M	M
519................	530	2.4	1.3	1.0–5.2	20.0–23.5	357	9030	. . .	. . .	M	NM?
526................	534	2.9	1.6	2.0–1.5	20.0–21.8	360	. . .	363	401	M	M
527................	535	1.6	4.3	1.4–3.0	21.2–22.5	2MASS	405	2MASS	10438	M	M
528................	537	2.8	3.0	2.6–3.1	22.3–22.7	364	400	373	. . .	M	M
540................	541	1.0	0.9	1.2–2.0	21.1–21.5	372	9037	375	9040	M	M
579................	580	2.2	1.8	1.7–2.4	21.7–22.2	396	423	400	. . .	M	M
583................	603	2.7	1.1	3.1–4.6	22.7–23.2	403	. . .	. . .	. . .	M	M
589................	590	2.1	1.4	3.7–3.1	23.3–22.6	. . .	. . .	408	. . .	NM?	M
621................	628	2.5	1.3	3.6–5.0	22.7–23.4	428	. . .	. . .	. . .	M	NM?
623................	629	1.7	1.0	2.8–2.3	22.5–22.5	429	9062	431	9064	M	M
655................	663	2.8	1.3	3.6–1.4	22.9–21.5	454	. . .	463	452	M	M
656................	670	2.6	1.2	3.9–1.5	23.3–21.6	. . .	. . .	466	454	NM	M
661................	662	2.6	1.4	1.5–4.5	20.0–23.2	457	9074	. . .	. . .	M	NM
668................	673	1.2	0.8	1.2–1.4	21.6–21.2	465	9077	467	9079	M	M
678................	681	2.4	1.2	4.1–4.5	22.9–23.2	. . .	. . .	. . .	. . .	NM	NM
682................	689	2.8	0.9	2.1–1.3	21.9–20.9	487	463	493	468	M	M
698................	699	0.8	1.3	1.4–1.5	21.1–21.6	499	9096	505	9096	M	M
705................	706	1.9	2.5	2.1–4.1	22.1–22.9	506	473	. . .	. . .	M	NM
707................	716	2.3	0.9	1.5–3.4	21.7–22.7	511	476	516	. . .	M	M
714................	722	1.7	4.0	1.2–1.3	21.5–21.4	510	. . .	520	. . .	M	M
725................	734	1.6	0.3	2.9–3.2	22.5–22.6	526	. . .	533	. . .	M	M
732................	744	2.2	0.6	1.3–1.3	21.0–21.3	535	1864	538	. . .	M	M
733................	746	1.6	0.4	2.5–2.2	22.5–22.1	531	. . .	542	488a	M	M
765................	777	1.6	0.8	3.2–2.4	22.6–22.9	567	. . .	574	9128	M	M
766................	778	1.0	0.6	1.6–1.1	21.5–21.4	565	1863b	573	1863a	M	M
768................	769	1.0	0.3	1.6–3.1	21.5–22.7	559	503	562	. . .	M	M
774................	782	2.2	2.5	1.5–1.6	21.6–22.0	576	506	584	9135	M	M
784................	806	2.8	1.5	3.5–4.9	22.7–23.3	586	511b	599	. . .	M	M
787................	788	2.6	0.4	2.4–1.5	22.4–22.1	585	512	582	. . .	M	M
820................	826	2.0	0.4	3.6–2.3	22.9–22.1	611	. . .	619	524	M	M
832................	842	2.0	1.3	1.3–1.3	21.5–21.3	628	529	634	9158	M	M
840................	861	2.4	2.2	1.5–3.7	21.2–22.8	636	. . .	. . .	. . .	M	NM
843................	854	2.6	1.1	2.7–1.4	22.7–21.2	630	. . .	642	536	M	M
844................	862	2.7	0.9	1.6–1.2	22.0–20.5	638	532	649	539	M	M
847................	856	3.0	0.1	1.4–1.5	21.6–21.6	640	534	644	537	M	M
884................	906	2.5	0.8	4.0–1.7	23.0–. . .	674	9181	691	9188	M	M
910................	922	1.6	0.5	1.1–1.3	21.3–21.2	698	9194	705	562	M	M
912................	913	1.7	0.2	1.9–1.5	22.1–21.8	700	9195	701	9196	M	M
917................	940	2.9	2.8	1.6–4.8	21.6–23.3	706	561	. . .	. . .	M	NM
943................	944	2.1	0.4	1.4–2.3	21.4–22.4	727	575	725	9210	M	M
977................	978	2.6	1.9	3.0–3.3	22.8–22.6	762	. . .	758	. . .	M	M
1049..............	1050	2.2	3.2	1.7–1.4	21.9–. . .	817	10561	816	10560	M	M

TABLE 3—*Continued*

X-RAY SOURCES						OPTICAL/NEAR-INFRARED SOURCES					
COUP (W) Number (1)	COUP (E) Number (2)	Separation (arcsec) (3)	Off-Axis (arcmin) (4)	MedE (W-E) (keV) (5)	log N_H (W-E) (cm^{-2}) (6)	IR (W) (7)	Opt. (W) (8)	IR (E) (9)	Opt. (E) (10)	Class (W) (11)	Class (E) (12)
1174................	1175	2.1	1.2	1.5–1.5	21.7–21.5	922	698	928	9292	M	M
1205................	1211	1.9	1.4	2.4–1.1	22.3–20.0	945	710	948	710h	M	M
1326................	1327	1.2	3.0	1.5–1.6	21.7–21.8	1068	777	1069	777	M	M
1392................	1393	2.4	3.6	3.0–2.5	22.6–22.2	1127	...	1125	...	M	M
1412................	1416	2.9	3.1	1.2–1.3	21.2–21.4	1146	830	1150	10667	M	M

NOTES.—Cols. (1)–(2): Source numbers of COUP sources within 3″ of each other. Col. (3): Component separation in arcsec. Col. (4): Off-axis angle in arcmin. Col. (5): Median energy of binary components in keV corrected for background. Col. (6): Logarithm of column density of binary components in cm^{-2}. Col. (7): Near-infrared counterpart in the VLT catalog of the first COUP component (M. J. McCaughrean et al. 2005, in preparation). Col. (8): Optical counterpart of the first COUP component (Hillenbrand 1997; Herbst et al. 2002). Col. (9): Near-infrared counterpart of the second COUP component. Col. (10): Optical counterpart of the second COUP component. Col. (11): Proposed class of the first COUP component (M = established member, NM = new member based on variability (§ 2.3), NM? = possible new member based on high source density (§ 2.4). Col. (12): Proposed class of the second COUP component. See Appendix for notes on individual objects.

2005), which uses the `max_likelihood.pro` procedure provided by the ASTRO library of the IDL software package.

As demonstrated by Scally et al. (1999), it is not easy to differentiate true physical binaries from unrelated cluster members in chance proximity. For 48 of the 61 COUP doubles, both components appear in the VLT JHK_s catalog (M. J. McCaughrean et al. 2005, in preparation). The physical reality of these doubles is best discussed in a future study of the full VLT sample. In 19 of these cases, both components have different bright optical counterparts in the Jones & Walker (1988) or Prosser et al. (1994) catalogs (optical star designations 0–9999) and thus were included in earlier ONC binarity studies (McCaughrean 2001).

To evaluate the importance of chance proximity, we performed Monte Carlo simulations of COUP source positions by randomly locating point sources within circular annuli of 0′.5 or 0′.25 width with the number of simulated sources equal to the COUP source counts in each annulus. Simulations show that, within the central 8′ area of the COUP field, the expected number of random pairs with separations <3″ ranges from 70 to 90. The observed and simulated off-axis angle and source separation distribution functions are also similar. Thus, chance proximity between physically unrelated COUP sources can explain the presence of all 61 COUP wide-double sources listed in Table 3. The difference between the 61 observed and 70–90 predicted chance pairs can be attributed to incompleteness in the COUP detection procedure in close proximity to bright X-ray sources.

We note, however, that 11 of the COUP doubles are new in the sense that one or both components have no counterpart in any optical or infrared survey. These are classified as "NM" or "NM?" in Table 3. The doubles COUP 589–590, 621–628, and 678–681 are potentially physical binaries because of similarities in the X-ray absorption in the spectra of the two components.

We conclude that, when X-ray/X-ray source doubles are considered, the COUP survey has uncovered no more than three, but quite possibly zero, new physical binary systems with separations between 0′′.7 and 3′′.0 (250–1000 AU projected separation). Forty-eight other doubles are independently found in COUP and in the new VLT merged near-infrared catalog of McCaughrean et al., but these are consistent with chance proximity of unrelated Orion stars.

4.2. *Additional Binary Findings*

When single COUP sources are examined for proximity to previously known stars, several additional noteworthy cases emerge.

In at least 8 cases, COUP has detected new sources proximate to known Orion cloud members, and some of these may be physical binaries. Five examples (COUP 599, 678, 683, 940, 1237) occur in the central part of the field, where VLT NIR counterparts reported in Getman et al. (2005) have unusually high positional offsets of >0′′.6. The complicated case of the massive, heavily obscured Becklin-Neugebauer (BN) Object is discussed by Grosso et al. (2005). Here an X-ray–bright new star (599 in the COUP catalog of Getman et al. but now designated COUP 599a) lies 0′′.9 from the BN Object, which appears to be coincident with a fainter X-ray source designated COUP 599b, which was not found in the standard processing of Getman et al. Similarly, we report here that COUP 683 is probably associated with a new companion to VLT 484 with 0′′.9 positional offset. COUP source 678 is probably a new deeply embedded star with log N_H = 22.9 cm^{-2} and not associated with VLT 476 with offset 0′′.9. COUP 940 was listed in Getman et al. (2005) as having the L-band counterpart FLWO 890 (Muench et al. 2002), but this match is unlikely with a positional offset of 1′′.3 (see footnote to Table 3).

Four additional likely new companions to known Orion members lie outside the VLT field of view. COUP 84 is a faint, lightly absorbed source lying 6′.5 off-axis. Its point spread function overlaps the $V \simeq 15$ G star JW 141, but with the X-ray centroid lying 5″ east of the star, it is probably a new low-mass companion or an unrelated star. Three bolometrically faint X-ray sources (COUP 400, 908, and 1238) are detected in the vicinity of three bright off-axis ONC members. J-band 2MASS images provide us with a hint for the presence of their very weak IR counterparts in the vicinity of bright primaries.

New low-mass companions around intermediate- and high-mass members of the ONC are found in the COUP data set. COUP source 1237 lies in the point spread function wings of the bright source COUP 1232 associated with the O9–B2 star θ^2 Ori A. This and similar sources, and the implication for X-ray emission from hot young stars, are discussed in a separate COUP study by Stelzer et al. (2005).

5. FIELD STARS

X-ray surveys are effective in discriminating old field stars from the cluster population due to the high X-ray emissivity of young stars (e.g., Feigelson & Lawson 2004). The ratio L_X/L_{bol} for the Orion population is typically a factor of 10^2–10^3 larger compared to that of 0.5–2 $M_\odot$ old disk stars, though the difference
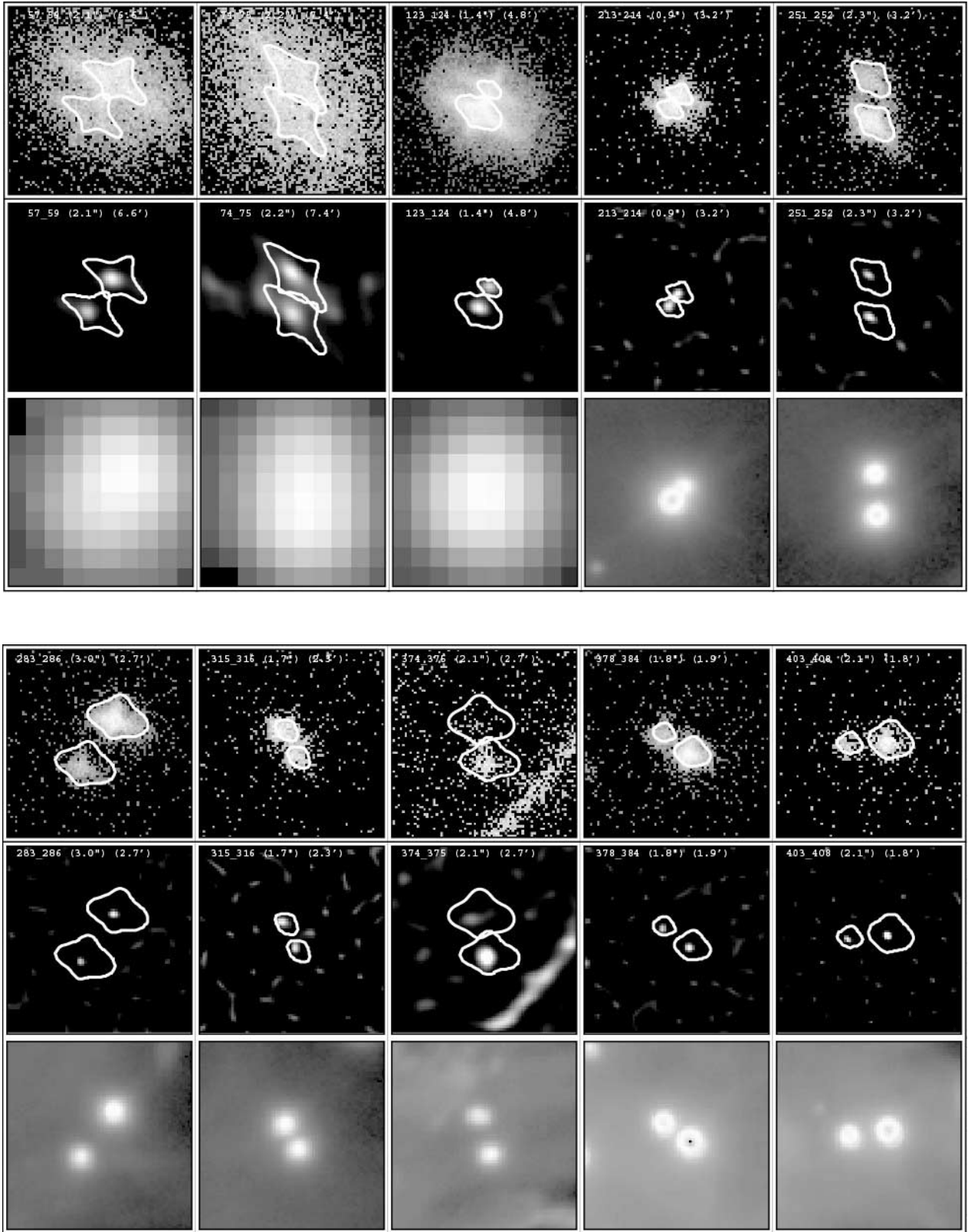
FIG. 4.—Three postage-stamp images for each of 61 COUP double sources with separations $<3''$: (top) $10'' \times 10''$ raw COUP image binned at high resolution with $0''.125$ pixel^{-1}; (middle) maximum likelihood reconstruction of the COUP data; and (bottom) K_s-band image from the Very Large Telescope or (for far-off axis sources) 2MASS surveys. Dark centers in some JHK_s stars are detector saturation effects. The labels give the COUP numbers of binary components, the component separation, and the off-axis angle. The closed curves show the extraction regions used in COUP analysis that are matched to the local *Chandra* point spread function and the proximity of the companion.
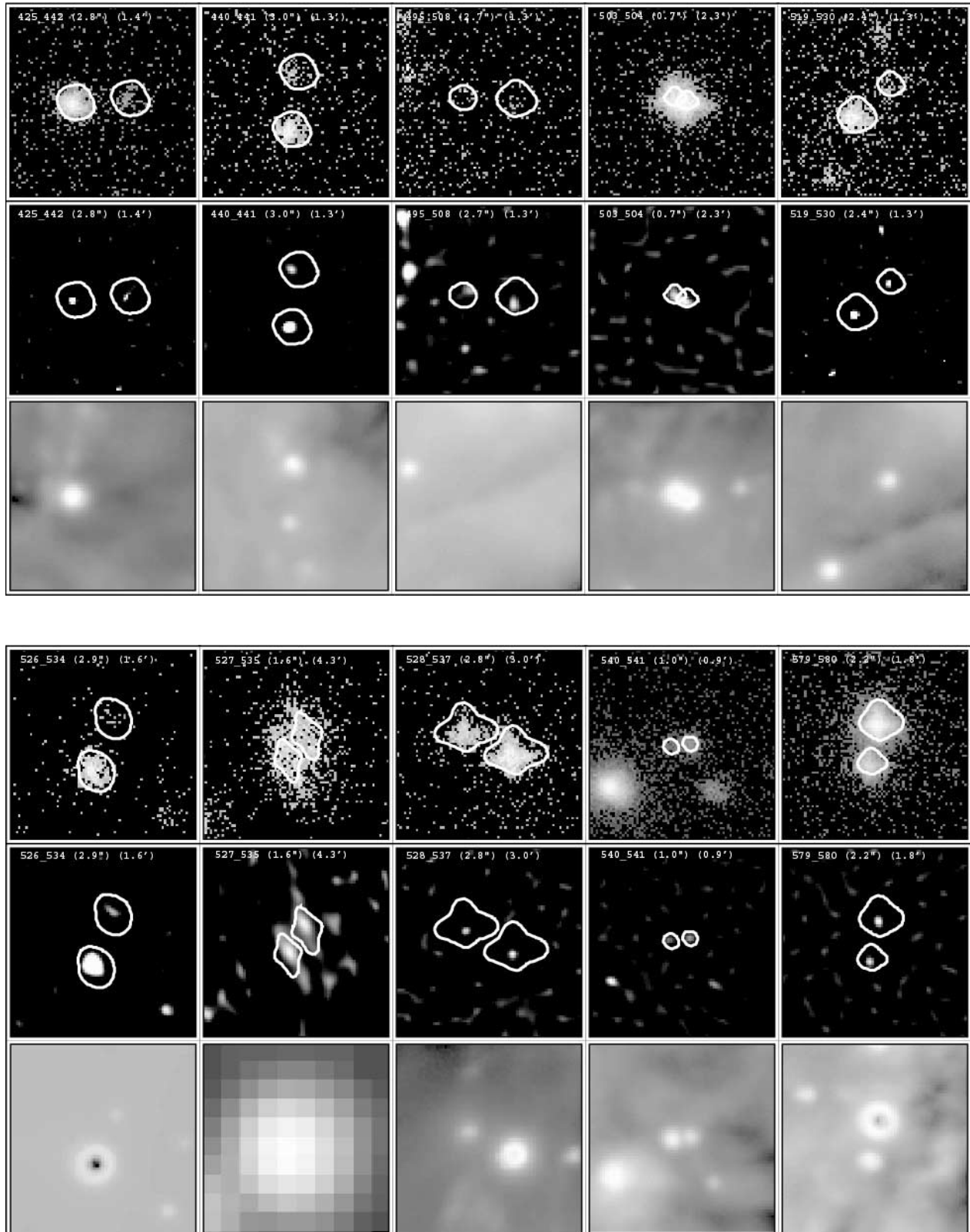
Fig. 4.—*Continued*

is smaller for younger ZAMS stars and for lower mass stars (Preibisch & Feigelson 2005; Preibisch et al. 2005). In the COUP field, the situation is confused by the wide range of obscuration: both Orion stars in the nebula region and foreground stars suffer little absorption, while both embedded Orion stars and back-ground disk stars are heavily absorbed. Many stars also do not have sufficient optical photometry and spectroscopy to directly obtain A_V and L_{bol}.

We proceed to examine COUP stars for possible field star candidates using three sources of information: the proper motion
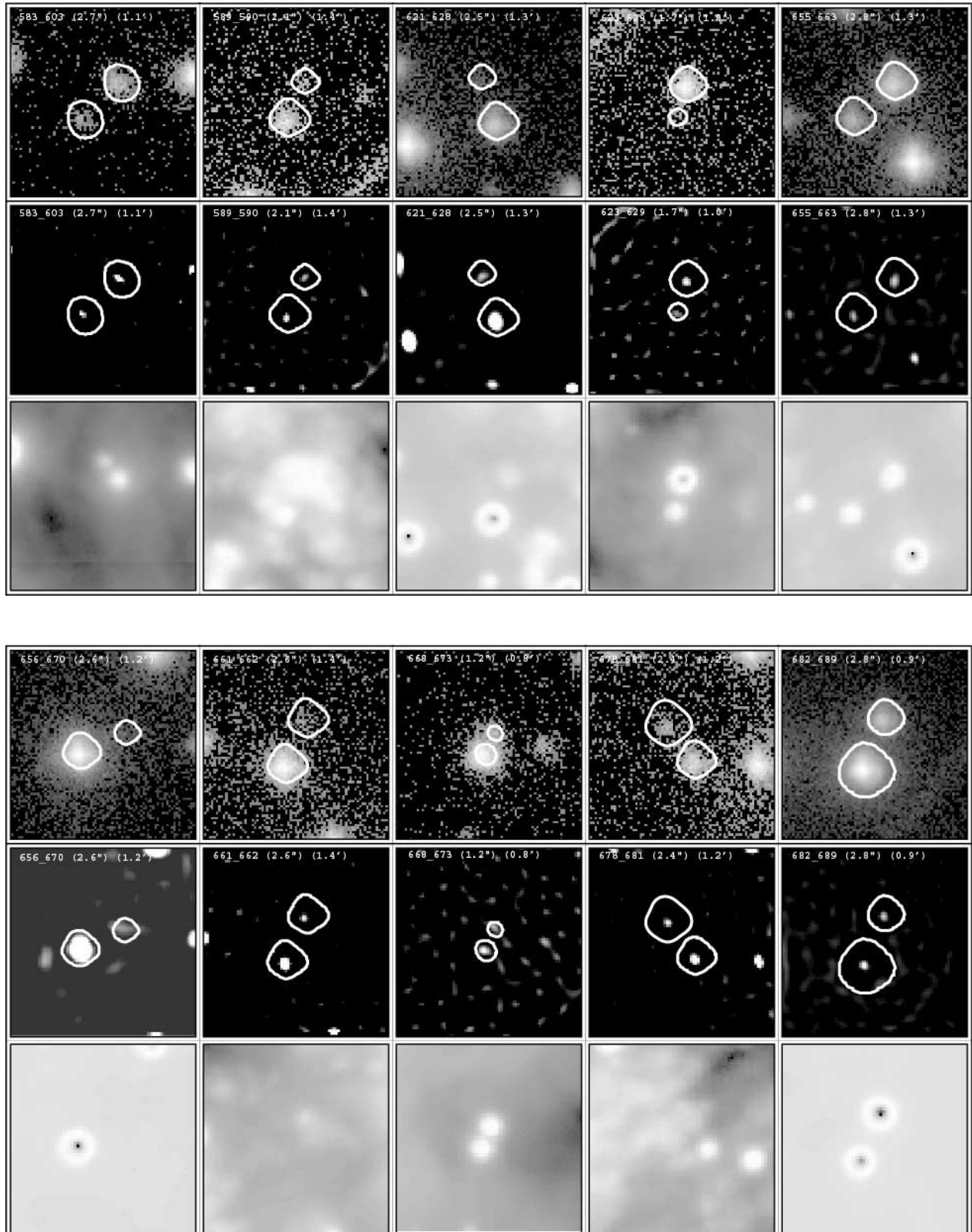
Fig. 4.—*Continued*

survey of Jones & Walker (1988); the JHK_s NIR colors from the VLT survey in the inner $7\overset{.}{'}4 \times 7\overset{.}{'}4$ region (M. J. McCaughrean 2005, in preparation) and the 2MASS survey in the outer region; and the Besançon stellar population synthesis model of the Galactic disk population (Robin et al. 2003).

First, we create a subsample of 33 COUP stars with proper motions inconsistent with cluster membership shown in Table 4. From the COUP optical sample of 977 stars, 35 COUP stars have membership probabilities $P < 90\%$ based on the proper motion study of Jones & Walker (1988). Two of them are omitted here:
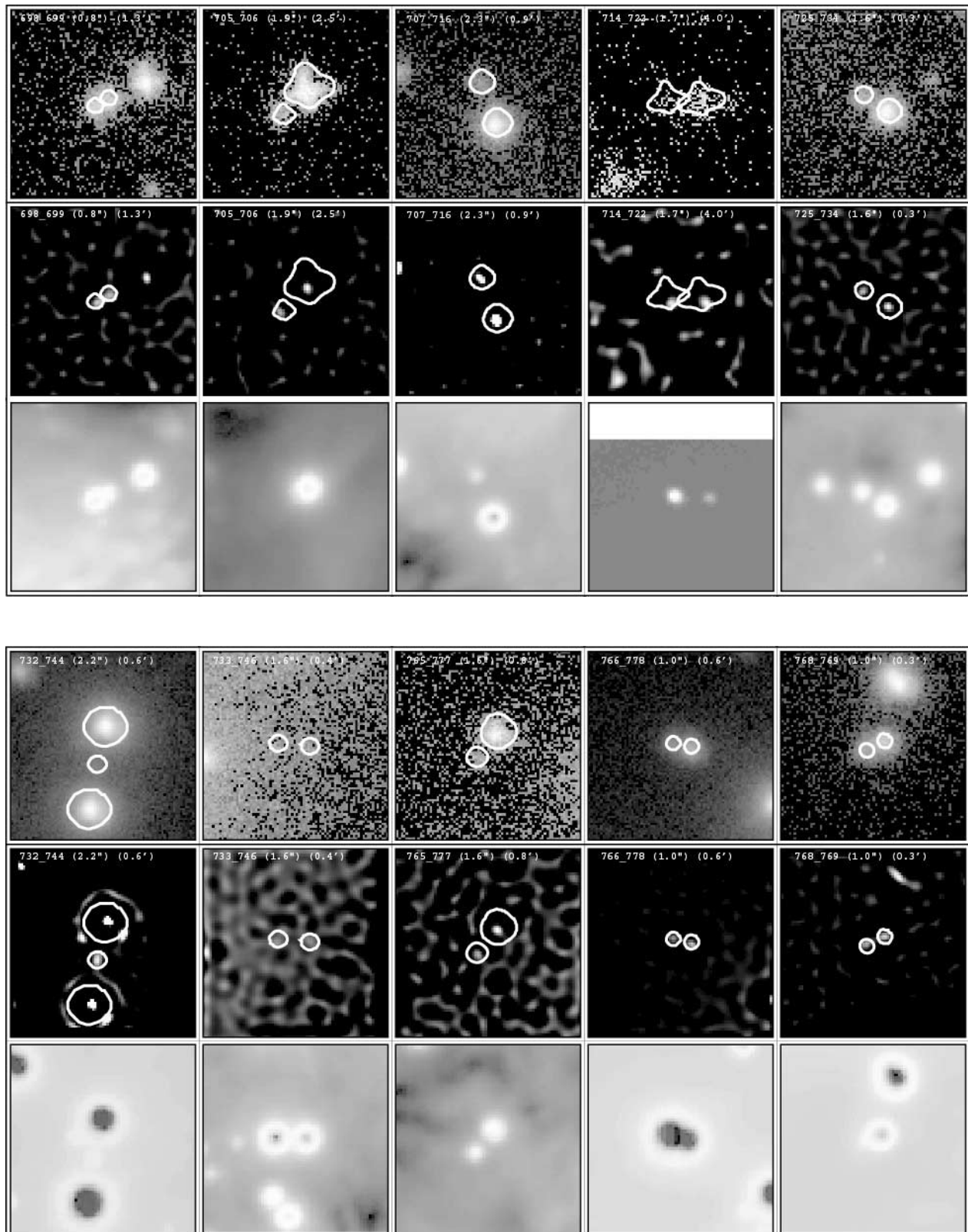
Fig. 4.—*Continued*

COUP 279, a $P = 22\%$ star with an imaged disk (proplyd) that is clearly a cluster member (Kastner et al. 2005); and COUP 1232 with $P = 80\%$, which is θ^2 Ori A, a O 9.5 star that is the second-most massive member of the Trapezium cluster (Stelzer et al. 2005).

Discrepant Jones & Walker (1988) proper motion measurements alone may not be a definitive indicator of nonmembership, as they are based on decades of photographic images that may be affected by binarity, disks, or dynamical events such as stellar ejection after close three-body encounters (Tan
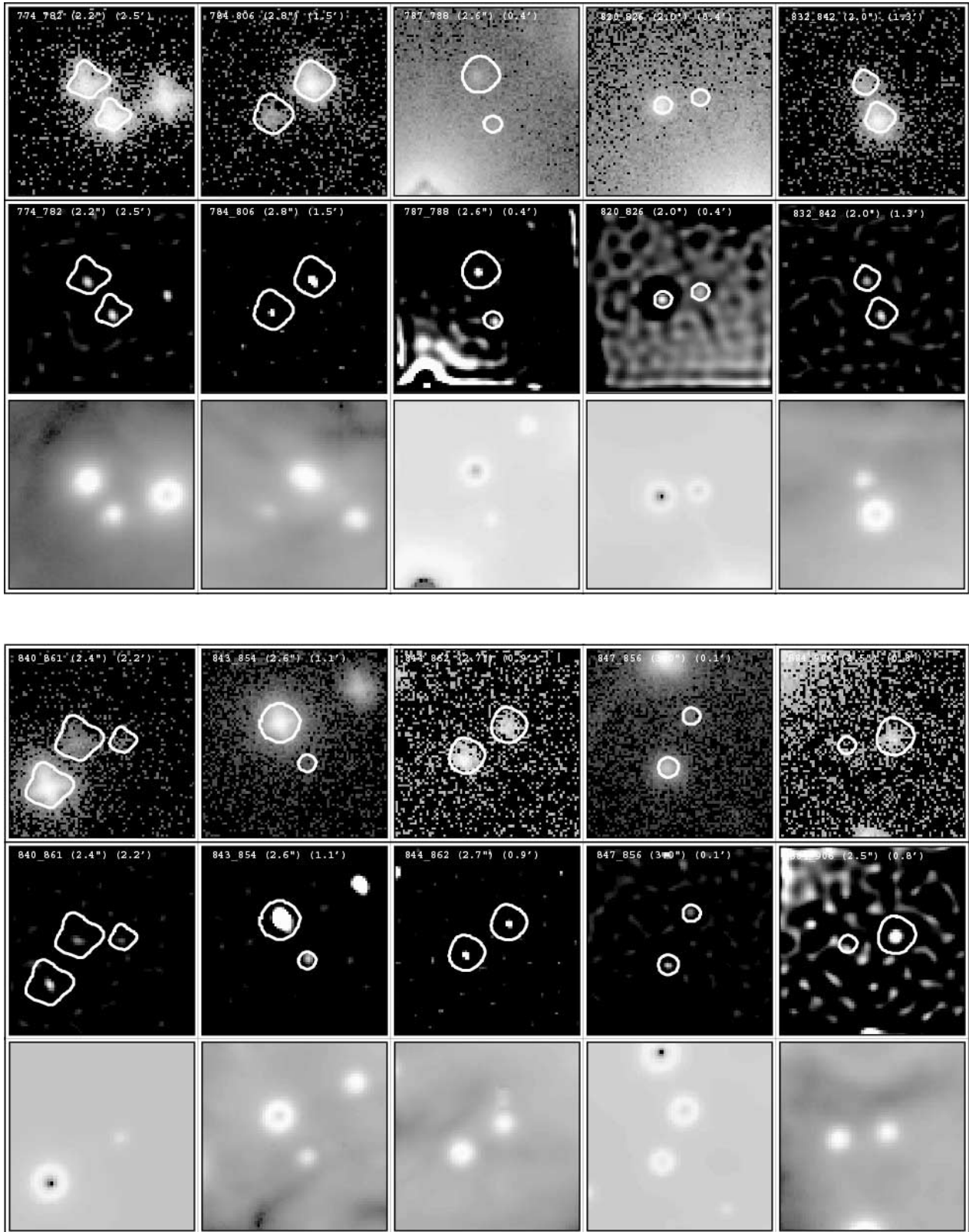
Fig. 4.—*Continued*

2004). We therefore combine NIR color information, shown in Figure 5, with proper motion measurements to select field star candidates from this subsample. We adopt the criterion that field stars should show little reddening ($J - H < 0.9$ roughly equivalent to $A_V < 2-3$) and should not exhibit K_s-band excesses attributable to circumstellar dust. Sixteen sources satisfying these criteria, most of which have very low proper motion membership probabilities ($P < 50\%$), are marked by an "F" in column (16) of Table 4. All except one have $K_s < 13$ mag.
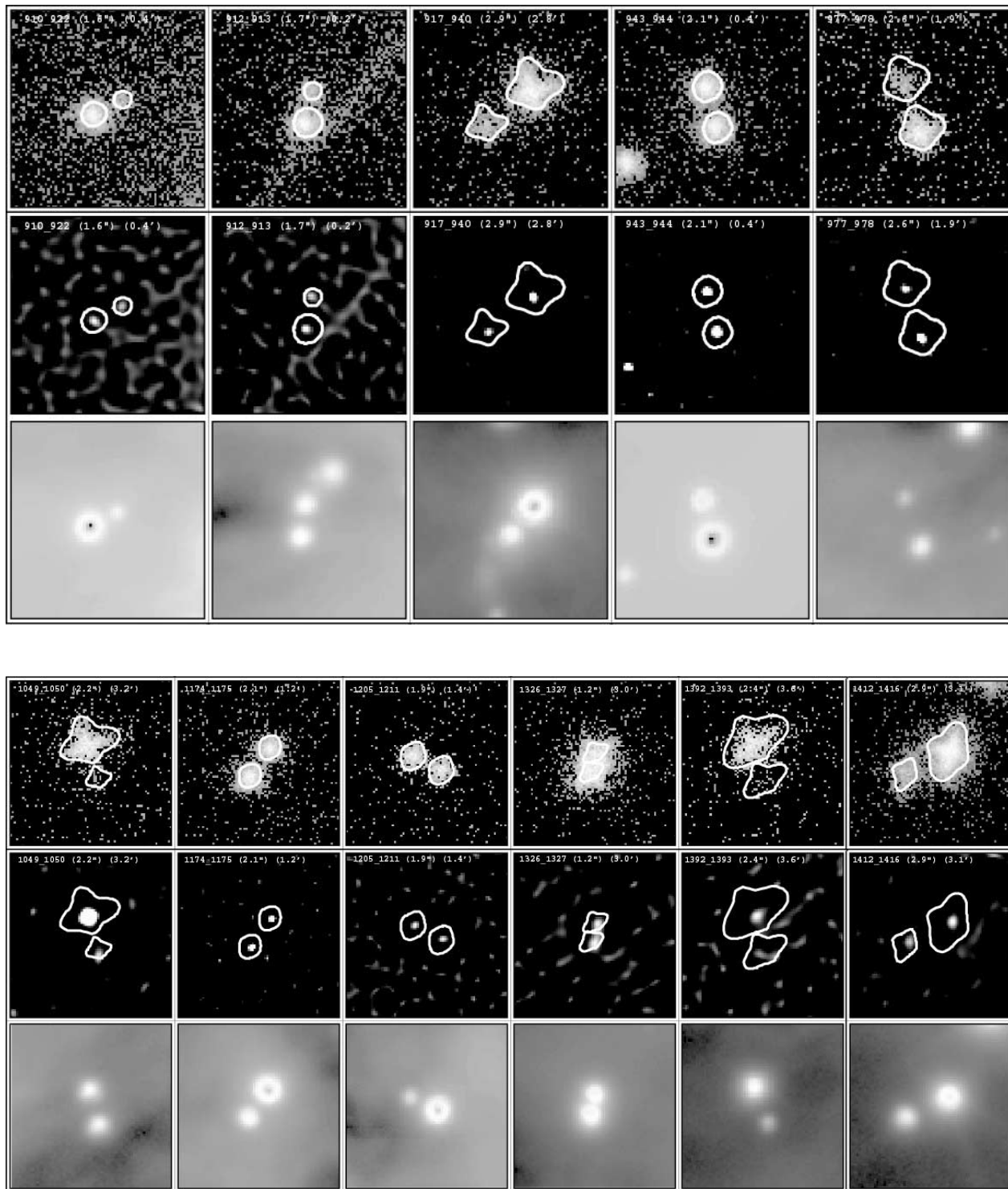
Fig. 4.—Continued

We supplement these 16 candidate X-ray–detected field stars with similar stars that are undetected in the COUP survey.[12] Adopting a limit $K_s < 13$, 159 bright stars (79 in the inner VLT survey region and 80 in the outer 2MASS region) are not detected in X-ray. The majority of those ($\sim$70%) are subject to factors that hinder X-ray detection: low local ACIS exposure

time, high local background due to readout streaks from bright ONC sources, and contamination from the point spread function wings of very nearby bright X-ray sources. In other cases, 2MASS sources have contamination flags and may be bright knots in the nebular emission rather than true stars. Requiring that the sources have JHK_s colors consistent with unreddened main-sequence stars (Bessell & Brett 1988), we find 6 X-ray–undetected $K_s < 13$ stars in the COUP field of view presented in Table 5. Thus, our sample of possible field stars with the limiting K_s of 13 mag consists of 22 stars, 16 with COUP detections

[12] We also checked the JHK_s color-color diagram for 356 COUP sources with IR but without optical counterparts and found that none of them lies at the locus of unreddened main-sequence stars. We consider them as likely cluster members.

TABLE 4
COUP Stars with Discrepant Proper Motions

COUP Number (1)	COUP J (2)	log N_H (cm^{-2}) (3)	L_t[a] (ergs s^{-1}) (4)	IR (5)	J (mag) (6)	H (mag) (7)	K_s (mag) (8)	JW (9)	V (mag) (10)	I (mag) (11)	A_V (mag) (12)	log L_t/L_{bol} (13)	P (14)	Spectral Type (15)	Field? (16)
2	053429.5−052354	21.2	30.34	05342924−0523567	10.19	9.78	9.61	5	12.0	11.0	0.3	−3.89	1	K1	F
7	053439.7−052425	20.9	31.01	05343976−0524254	8.85	8.10	7.95	45	11.4	9.9	0.8	−3.77	0	K1−K4	F
127	053458.0−052940	21.4	28.27	05345805−0529405	13.92	12.85	12.26	182	...	16.6	...	...	48	...	...
153	053501.1−052955	21.2	27.82	05350116−0529551	12.87	12.24	12.03	209	16.8	14.2	...	...	0	...	F
188	053503.0−053001	21.3	30.89	05350299−0530015	10.33	9.51	9.22	232	13.6	11.7	2.2	−3.52	79	K1−K2	F
267	053506.4−053335	20.0	30.50	05350644−0533351	11.01	9.68	8.72	295	15.7	13.9	0.0	−2.53	0	M0.5e−M2	...
378	053510.4−052245	21.1	30.11	238	10.75	9.84	9.49	345	14.8	12.4	1.3	−3.85	81	M0−M2	...
492	053512.7−052034	21.9	29.48	340	13.40	12.18	11.49	389	19.5	15.9	0.5	−3.18	52	M4.5−M6	...
561	053513.6−051954	22.1	30.78	387	11.12	9.41	8.34	413	...	14.6	0.0	−1.94	0	K5	...
645	053514.6−052042	22.1	30.23	442	11.57	9.88	9.01	445a	18.9	14.7	...	...	26	Cont.	...
669	053514.9−052159	21.5	30.76	472	10.92	10.06	9.76	457	14.5	12.5	2.0	−3.25	79	K3−K4	F
672	053514.9−052339	21.4	30.46	470	10.65	9.80	9.43	456	14.6	12.2	...	...	4	...	F
743	053515.8−052301	21.5	29.29	546	11.34	10.34	9.66	494	15.9	13.6	2.0	−4.36	0	K7	...
756	053515.9−052221	21.6	29.33	552	12.28	10.92	9.95	496	17.0	14.2	3.0	−4.30	0	K7e	...
813	053516.5−052405	21.5	30.05	608	11.87	11.05	10.63	521	18.5	14.3	6.1	−4.30	86	M0	F
922	053517.8−052315	21.2	29.57	705	11.15	10.21	9.77	562	15.7	13.0	2.2	−4.37	17	M0	...
939	053518.0−051613	22.1	30.58	05351799−0516136	11.49	9.97	8.86	566	18.7	14.9	...	...	0	...	...
949	053518.2−051306	22.1	30.11	05351822−0513068	11.48	10.30	9.64	572	17.2	13.9	...	...	81	...	...
958	053518.2−052535	20.0	27.57	736	13.23	12.65	12.39	583	16.2	14.5	0.0	−5.25	0	M1	F
994	053518.8−051445	21.5	30.15	05351883−0514455	12.21	11.31	10.89	597	16.8	14.0	...	...	0	...	F
1111	053520.6−052353	21.4	30.37	869	11.84	11.07	10.66	659	18.2	14.0	...	...	84	...	F
1122	053520.9−052150	21.5	30.05	882	11.82	10.66	9.89	665	15.5	13.7	...	...	9	M:e	...
1158	053521.6−052147	21.9	30.49	914	11.90	10.54	9.70	687a	17.7	14.7	2.7	−2.90	54	M1:	...
1326	053525.4−052134	21.7	29.60	1068	12.72	11.40	10.58	777	18.5	15.1	4.8	−4.08	80	K6	...
1327	053525.4−052135	21.8	29.76	1069	12.04	10.96	10.60	777	18.5	15.1	4.8	−3.92	80	K6	...
1336	053525.7−052641	21.8	29.86	1077	12.02	10.94	10.29	786	16.3	13.9	1.3	−3.50	89	M0−M1	...
1373	053526.9−052448	21.1	28.75	1105	13.36	12.59	12.23	806	...	15.2	0.0	−4.28	0	M6.5	F
1485	053532.0−051620	22.0	29.82	05353199−0516201	12.81	11.76	11.23	879	16.7	14.4	...	...	0	≤M1	...
1512	053534.3−052659	20.6	29.29	05353437−0526596	13.03	12.33	11.96	902	...	15.3	...	...	84	...	F
1537	053537.3−052641	20.0	28.89	05353738−0526416	10.63	10.02	9.84	928	13.6	11.7	...	...	0	...	F
1558	053540.5−052701	20.0	28.81	05354049−0527018	11.65	11.25	11.16	950	13.1	12.2	...	...	0	...	F
1569	053542.0−052005	20.0	28.84	05354209−0520058	14.20	13.59	13.33	958	18.7	15.7	0.3	−3.70	0	M4	F
1613	053556.8−052527	21.8	28.14	05355672−0525263	13.15	12.53	12.48	1037	15.2	13.9	0.0	−4.84	0	K5	F

Notes.—Cols. (1)–(2) give the COUP source number and COUP CXO name. Cols. (3)–(4) give column density and observed source luminosity (calculated assuming $d = 450$ pc, which will be incorrect for field stars) inferred from X-ray spectral fits. Cols. (5)–(8) present the NIR counterpart and its JHK_s photometry. For the inner region, these are from the VLT merged catalog of M. J. McCaughrean et al. (2005, in preparation), while for the outer region they are from the 2MASS catalog. Cols. (9)–(12) give the optical counterpart identifier from the Jones & Walker (1988) survey, VI photometry and visual extinction from Hillenbrand (1997). Col. (13) gives the X-ray emissivity log L_t/L_{bol} in the total 0.5–8 keV band from Getman et al. (2005). Col. (14) lists the proper motion membership probability from Jones & Walker (1988). Col. (15) gives the spectral type from the optical spectroscopy of Hillenbrand (1997) updated as described in Getman et al. (2005). The final column gives the indicator of field star candidates suggested by our analysis.

[a] The value of L_t was calculated assuming distance of 450 pc, which will be incorrect for field stars.
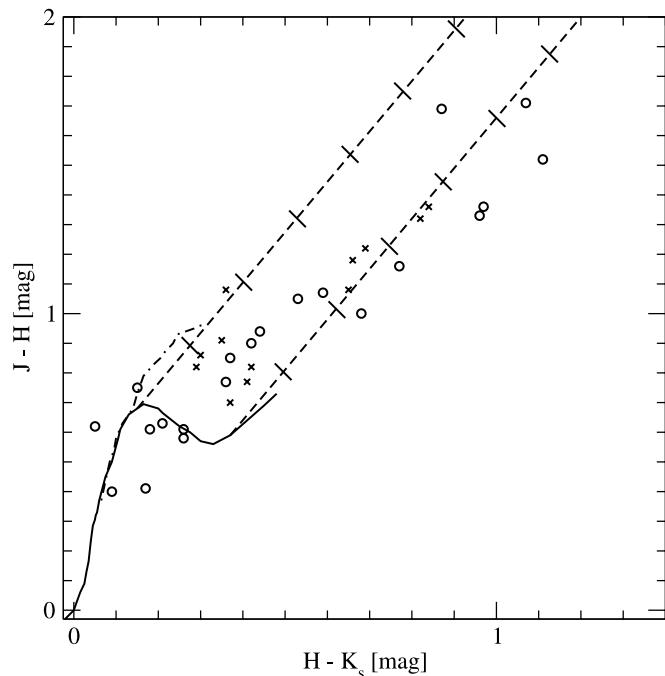
Fig. 5.—Near-infrared color-color diagram of 33 COUP sources with cluster membership probabilities $P < 90\%$ based on proper motions. Sixteen lie close to the locus of unreddened main-sequence stars ($J - H < 0.9$). Circles indicate sources with $P < 50\%$. The solid and dot-dashed curves show sites of intrinsic JHK_s colors of main-sequence and giant stars, respectively. The dashed lines are reddening vectors originating at M0 V (*left line*) and M6.5 V (*right line*), and marked at intervals of $A_V = 2$ mag.

Fig. 6.—K_s-band distribution functions for 22 suggested field star candidates (*gray bars*), including both detected and undetected stars in the COUP survey, and 23 field stars predicted from the Besançon stellar population synthesis model (*dashed histogram*).

The number, brightness distribution, and other properties of the predicted and candidate field star population are consistent with each other. However, in light of the large number of stars in the field excluded from consideration here (due to proximity of nearby X-ray–bright stars), the stars listed in Tables 4 and 5 can only be considered suggestions rather than clear identifications.

marked with an "F" in Table 4, and 6 without COUP detection listed in Table 5.

This sample of 22 field star candidates is compatible with the predictions of the stellar population synthesis model of the Galaxy for the sky position of the Orion region out to a distance of 450 pc (Robin et al. 2003).[13] The model predicts about 23 foreground stars with $K_s < 13$ mag in the COUP field of view. All except $\simeq 2$ are expected to be main-sequence dwarfs: about 10% A–F stars, 20% G stars, 50% K stars, and 20% M stars. Two-thirds of the simulated field stars have ages greater than 2 Gyr with the remaining ages ranging from 0.15 to 2 Gyr. About 60% of simulated field stars occupy the volume between 300 and 450 pc. The K_s-band distribution of the predicted 23 field stars are compared to the distribution for our 22 candidate field stars in Figure 6.

6. SUMMARY

The COUP observation provides an exceptionally deep X-ray survey of the nearest rich young (age ~ 1 Myr) stellar cluster, the Orion Nebula Cluster and associated embedded young stellar objects. Membership of the region is important for studies of the stellar IMF, cluster dynamics, and star formation. ONC membership has been intensively investigated at ONIR wavelengths. COUP provides the best opportunity to examine the benefits and limitations of X-ray selection to such membership studies. In addition to straightforward associations of X-ray sources with ONIR stars, we have evaluated the levels of contamination by stellar and extragalactic sources unrelated to the Orion star-forming cloud using detailed simulations of X-ray–emitting populations. Our main findings are as follows:

1. A total of 1331 COUP sources have ONIR counterparts. Except for about 16 suggested field stars unrelated to the Orion cloud (Table 4), all of these are true members of the ONC or are obscured members of the background molecular cloud. Only 16 of those sources (Table 4, marked with an "F") with discrepant proper motions are suggested field stars based on a stellar population synthesis model of the Galactic disk.

[13] The Monte Carlo simulation of the stellar population in the cone subtended by the COUP field was computed with the Web service provided by the Besançon group at http://bison.obs-besancon.fr/modele/.

TABLE 5
SUGGESTED FIELD STARS UNDETECTED IN COUP

2MASS	CR_u	JW	P	V	I	J	H	K_s	Remarks
05343359−0523099	0.092	...	...	...	...	11.28	10.78	10.72	0″7 from JW23 with P=0
05350458−0528266	0.035	255	0	15.36	13.94	13.07	12.45	12.30	Par 1738
05352631−0515113	0.067	794	0	11.67	10.86	10.23	9.78	9.72	Par 2021; G9 IV–V
05353053−0531559	0.076	858	0	18.03	15.60	13.82	13.07	12.72	...
05353249−0529021	0.164	889	0	14.43	13.34	12.68	12.15	12.02	Par 2098
05354007−0527589	0.166	947	64	17.02	14.36	12.97	12.45	12.17	M2:

NOTES.—Count rate upper limits CR_u are in counts ks^{-1} from Getman et al. (2005). Membership probabilities are from Jones & Walker (1988). VI photometry is from Hillenbrand (1997), JHK_s photometry is from 2MASS, and spectral types are from Hillenbrand (1997).

2. The long exposure of COUP optimizes the chance of capturing powerful X-ray flares and thereby distinguishing absorbed young stellar objects from the background Galactic or extragalactic populations. We found that 42 heavily absorbed sources without ONIR identifications exhibit one or more high-amplitude X-ray flares, which convincingly demonstrates that they are newly discovered Orion cloud members (Table 1). They are all heavily absorbed, and almost all are spatially associated with the two well-known OMC-1 cores and the dense molecular filament, which extends northward from OMC-1 to OMC-2/3. Thirty-three additional obscured COUP sources that do not exhibit X-ray flares lie in this region and are also likely to be OMC members (Table 2, marked as "OMC or EG?").

3. Based on detailed simulations of the extragalactic background population, including instrumental background and obscuration effects by the molecular cloud, we find that about 159 COUP sources are probably extragalactic AGNs unrelated to the Orion star-forming region (Table 2, EG).

4. We find 16 lightly obscured sources without ONIR counterparts, likely new members of the Orion Nebular Cluster (ONC in Table 2). Some are close neighbors of bright Orion stars.

5. Among unidentified sources we see two in which the X-ray emission is unusually soft, constant, and faint and is associated with a nebular shock rather than a star (Table 2, HH). These and possible other similar sources will be studied in detail by N. Grosso et al. (2005, in preparation).

6. A total of 122 COUP sources lie within $3''$ of another COUP source, forming 61 apparent double sources. Simulations indicate that most of these are random pairings rather than physical wide binaries. Eleven of these doubles are new with one or both components not previously found in ONIR studies.

Facilities: CXO (ACIS)

APPENDIX

NOTES ON INDIVIDUAL OBJECTS

COUP 57–59.—These sources lie outside the VLT survey field of view. The corresponding 2MASS source 05345071−0524014 is an unresolved blend of these two stars.

COUP 74–75.—These sources lie outside the VLT survey field of view. The corresponding 2MASS source 05345275−0527545 is an unresolved blend of these two stars.

COUP 123–124.—These sources lie outside the VLT survey field of view. The corresponding 2MASS source 05345766−0523522 is an unresolved blend of these two stars.

COUP 315–316.—These sources are unlikely to be a physical binary due to the large difference in X-ray absorption and optical brightness.

COUP 425–442.—These sources are unlikely to be a physical binary due to the large difference in X-ray absorption and optical brightness. Neither K_s-band nor optical band images detect the highly absorbed component, which is a flaring X-ray source (COUP 425).

COUP 495–508.—The VLT survey did not detect either of these two faint COUP sources, possibly due to strong nebula emission in the region. The sources are unlikely to be a physical binary due to the large difference in X-ray absorption.

COUP 519–530.—VLT did not detect the X-ray brighter, but highly absorbed component (COUP 530). These sources are unlikely to be a physical binary due to the large difference in X-ray absorption and optical brightness.

COUP 527–535.—These sources lie outside the VLT survey field of view; the corresponding 2MASS source 05351324−0527541 is an unresolved blend of these two stars. The COUP stars are detected and resolved in optical catalogs.

COUP 583–603.—The highly absorbed component of this X-ray double (COUP 603) was not detected in the VLT survey but is source 151 in the *L*-band survey of Lada et al. (2004). The VLT image has a third source, VLT 403, located $\simeq 1''$ northeast of COUP 583.

COUP 589–590.—The southern component COUP 590 lines in a bright extended region in the VLT K_s-band image.

COUP 621–628.—The VLT did not detect the northern, highly absorbed component of this visual binary (COUP 628). Another K_s-band object, possibly a nebular knot, located $\simeq 2''$ northwest of VLT 428 is not associated with any COUP source.

COUP 656–670.—The VLT did not detect the highly absorbed component of this visual binary (COUP 656). These sources are unlikely to be a physical binary due to the large difference in X-ray absorption and optical brightness.

COUP 661–662.—The VLT did not detect the highly absorbed, X-ray flaring component of this visual binary (COUP 662). These sources are unlikely to be a physical binary due to the large difference in X-ray absorption and optical brightness.

COUP 678–681.—These highly absorbed components lie in a region of bright K_s-band nebulosity. Getman et al. (2005) associate COUP 678 with the star VLT 476 with offset of $0\rlap{.}''9$ based on their automated identification procedure. But, from examination of the images here, we suggest that this offset is too large to be instrumental and that the association is incorrect. We thus include COUP 678, which exhibits X-ray flares, in Table 1 as a new obscured member of the Orion region.

COUP 705–706.—VLT did not detect the highly absorbed, X-ray flaring component of this visual binary (COUP 706). These sources are unlikely to be a physical binary due to the large difference in X-ray absorption and optical brightness.

COUP 732–744.—Together with COUP 745 $\simeq 3''$ southeast of 744, these sources comprise an apparent triple system with K_s-band counterparts VLT 535–538–540. VLT resolved the northwest component into another double, VLT 535(= COUP 732) and VLT 545 with separation $0\rlap{.}''1$, too close to be resolved by *Chandra*. These X-ray sources are sufficiently bright that errors in the image reconstruction technique are visible as rings in the middle panel of Fig. 4.

COUP 766–778.—These sources correspond to θ^1 Ori BE and θ^1 Ori BW and are discussed in detail by Stelzer et al. (2005).

COUP 768–769.—These sources are unlikely to be a physical binary due to the large difference in X-ray absorption and optical brightness.

COUP 840–861.—The VLT did not detect highly absorbed, X-ray flaring component of this double (COUP 861). These sources are unlikely to be a physical binary due to the large difference in X-ray absorption.

COUP 917–940.—Optical band and VLT K_s band images did not detect the highly absorbed, X-ray flaring component of this visual binary (COUP 940). However, the VLT resolves a third star (VLT 712) between the two *Chandra* sources. The automated identification procedure of Getman et al. (2005) associated COUP 940 with *L*-band source FLWO 890 (Muench et al. 2002). This is probably incorrect as FLWO 890 is more likely associated with the K_s-band source VLT 712. Thus, COUP 940, which exhibits X-ray flares, is classified here as a new Orion cloud member without optical or IR counterpart.

REFERENCES

Bally, J., O'Dell, C. R., & McCaughrean, M. J. 2000, AJ, 119, 2919
Bally, J., Stark, A. A., Wilson, R. W., & Langer, W. D. 1987, ApJ, 312, L45
Barger, A. J., Cowie, L. L., Brandt, W. N., Capak, P., Garmire, G. P., Hornschemeier, A. E., Steffen, A. T., & Wehner, E. H. 2002, AJ, 124, 1839
Bauer, F. E., et al. 2003, Astron. Nachr., 324, 175
Bessell, M. S., & Brett, J. M. 1988, PASP, 100, 1134
Brandt, W. N., et al. 2001, AJ, 122, 2810
Duquennoy, A., & Mayor, M. 1991, A&A, 248, 485
Favata, F., Flaccomio, E., Reale, F., Micela, G., Sciortino, S., & Feigelson, E. D. 2005, ApJS, 160, 469
Feigelson, E. D., Broos, P., Gaffney, J. A., Garmire, G., Hillenbrand, L. A., Pravdo, S. H., Townsley, L., & Tsuboi, Y. 2002a, ApJ, 574, 258
Feigelson, E. D., & Lawson, W. A. 2004, ApJ, 614, 267
Flaccomio, E., Damiani, F., Micela, G., Sciortino, S., Harnden, F. R., Murray, S. S., & Wolk, S. J. 2003, ApJ, 582, 382
Getman, K. V., et al. 2005, ApJS, 160, 319
Grosso, N., et al. 2005, ApJS, 160, 530
Hambarian, V. V. 1988, Astrofizika, 28, 149
Herbst, W., Bailer-Jones, C. A. L., Mundt, R., Meisenheimer, K., & Wackermann, R. 2002, A&A, 396, 513
Hillenbrand, L. A. 1997, AJ, 113, 1733
Hillenbrand, L. A., & Carpenter, J. M. 2000, ApJ, 540, 236
Jones, B. F., & Walker, M. F. 1988, AJ, 95, 1755
Kastner, J., Franz, G., Grosso, N., Bally, J., McCaughrean, M., Getman, K. V., Feigelson, E. D., & Schulz, N. S. 2005, ApJS, 160, 511
König, B., Neuhäuser, R., & Stelzer, B. 2001, A&A, 369, 971
Kroupa, P., Petr, M. G., & McCaughrean, M. J. 1999, NewA, 4, 495
Kurtz, S., Cesaroni, R., Churchwell, E., Hofner, P., & Walmsley, C. M. 2000, in Protostars and Planets IV, ed. V. Mannings et al. (Tucson: Univ. Arizona Press), 299
Lada, C. J., Muench, A. A., Lada, E. A., & Alves, J. F. 2004, AJ, 128, 1254

Lucy, L. B. 1974, AJ, 79, 745
Makarov, V. V. 2002, ApJ, 576, L61
McCaughrean, M. J. 2001, in IAU Symp. 200, The Formation of Binary Stars, ed. H. Zinnecker & R. D. Mathieu (Dordrecht: Rediel), 169
Moretti, A., Campana, S., Lazzati, D., & Tagliaferri, G. 2003, ApJ, 588, 696
Muench, A. A., Lada, E. A., Lada, C. J., & Alves, J. 2002, ApJ, 573, 366
O'Dell, C. R. 2001, ARA&A, 39, 99
Padgett, D. L., Strom, S. E., & Ghez, A. 1997, ApJ, 477, 705
Paolillo, M., Schreier, E. J., Giacconi, R., Koekemoer, A. M., & Grogin, N. A. 2004, ApJ, 611, 93
Petr, M. G., Coude Du Foresto, V., Beckwith, S. V. W., Richichi, A., & McCaughrean, M. J. 1998, ApJ, 500, 825
Pravdo, S. H., Feigelson, E. D., Garmire, G., Maeda, Y., Tsuboi, Y., & Bally, J. 2001, Nature, 413, 708
Pravdo, S. H., Tsuboi, Y., & Maeda, Y. 2004, ApJ, 605, 259
Preibisch, T., & Feigelson, E. D. 2005, ApJS, 160, 390
Preibisch, T., et al. 2005, ApJS, 160, 401
Prosser, C. F., Stauffer, J. R., Hartmann, L., Soderblom, D. R., Jones, B. F., Werner, M. W., & McCaughrean, M. J. 1994, ApJ, 421, 517
Robin, A. C., Reylé, C., Derrière, S., & Picaud, S. 2003, A&A, 409, 523
Scally, A., Clarke, C., & McCaughrean, M. J. 1999, MNRAS, 306, 253
Slesnick, C. L., Hillenbrand, L. A., & Carpenter, J. M. 2004, ApJ, 610, 1045
Stelzer, B., et al. 2005, ApJS, 160, 557
Stolovy, S. R., et al. 1998, ApJ, 492, L151
Tan, J. C. 2004, ApJ, 607, L47
Vuong, M. H., Montmerle, T., Grosso, N., Feigelson, E. D., Verstraete, L., & Ozawa, H. 2003, A&A, 408, 581
Wolk, S. J., Harnden, F. R., Jr., Flaccomio, E., Micela, G., Favata, F., Shang, H., Glassgold, A., & Feigelson, E. D. 2005, ApJS, 160, 423
Zapata, L. A., Rodríguez, L. F., Kurtz, S. E., O'Dell, C. R., & Ho, P. T. P. 2004, ApJ, 610, L121